

000  
001  
002  
003  
004  
005  
006  
007  
008  
009  
010  
011  
012  
013  
014  
015  
016  
017  
018  
019  
020  
021  
022  
023  
024  
025  
026  
027  
028  
029  
030  
031  
032  
033  
034  
035  
036  
037  
038  
039  
040  
041  
042  
043  
044  
045  
046  
047  
048  
049  
050  
051  
052  
053  

# COST-AWARE STOPPING FOR BAYESIAN OPTIMIZATION

**Anonymous authors**

Paper under double-blind review

**ABSTRACT**

In automated machine learning, scientific discovery, and other applications of Bayesian optimization, deciding when to stop evaluating expensive black-box functions in a cost-aware manner is an important but underexplored practical consideration. A natural performance metric for this purpose is the *cost-adjusted simple regret*, which captures the trade-off between solution quality and cumulative evaluation cost. While several heuristic or adaptive stopping rules have been proposed, they lack guarantees ensuring stopping before incurring excessive function evaluation costs. We propose a *principled cost-aware stopping rule* for Bayesian optimization that adapts to varying evaluation costs without heuristic tuning. Our rule is grounded in a theoretical connection to state-of-the-art cost-aware acquisition functions, namely the Pandora’s Box Gittins Index (PBGI) and log expected improvement per cost (LogEIPC). We prove a theoretical guarantee bounding the expected cost-adjusted simple regret incurred by our stopping rule when paired with either acquisition function. Across synthetic and empirical tasks, including hyperparameter optimization and neural architecture size search, pairing our stopping rule with PBGI or LogEIPC usually matches or outperforms other acquisition-function-stopping-rule pairs in terms of cost-adjusted simple regret.

**1 INTRODUCTION**

Bayesian optimization is a framework designed to efficiently find approximate solutions to optimization problems involving expensive-to-evaluate black-box functions, where derivatives are unavailable. Such problems arise in applications like hyperparameter tuning (Snoek et al., 2012), robot control optimization (Martinez-Cantin, 2017), and material design (Zhang et al., 2020). It works by iteratively, (a) forming a probabilistic model of the black-box objective function based on data collected thus far, then (b) optimizing an acquisition function, which balances exploration-exploitation tradeoffs, to carefully choose a new point at which to observe the unknown function in the next iteration.

In this work, we consider the *cost-aware* setting, where one must pay a cost to collect each data point, and study *adaptive stopping rules* that choose when to stop the optimization process. After stopping at some terminal time, we measure performance in terms of simple regret, which is the difference in value between the best solution found so far and the global optimum. Collecting a data point can reduce simple regret, but incurs cost in order to do so.

As an example, consider using a cloud computing environment to tune the hyperparameters of a classifier in order to optimize a performance metric on a given test set. Training and evaluating test error takes some number of CPU or GPU hours, that may depend on the hyperparameters used. These come with a financial cost, billed by the cloud computing provider, which define our cost function. The objective value is the business value of deploying the trained model under the given hyperparameters—a given function of the model’s accuracy. From this perspective, simple regret can be understood as the opportunity cost for deploying a suboptimal model instead of the optimal one. Motivated by the need to balance cost-performance tradeoff in examples such as above, we aim to design stopping rules that optimizes *expected cost-adjusted simple regret*, defined as the sum of simple regret and the cumulative cost of data collection.

Several stopping rules have been proposed for Bayesian optimization. Simple heuristics—such as fixing a maximum number of iterations or stopping when the best value remains unchanged for a certain number of iterations—are widely used in practice, but can either stop too early or lead to unnecessary evaluations. Other approaches include acquisition-function-based rules that stop

when, for instance, the probability of improvement, expected improvement, or knowledge gradient drop below a preset threshold (Lorenz et al., 2015; Nguyen et al., 2017; Frazier & Powell, 2008); and regret-bound-based rules, which use theoretical performance guarantees to decide termination (Makarova et al., 2022; Ishibashi et al., 2023; Wilson, 2024). Most of these target the classical setting which does not explicitly incorporate function evaluation costs.

In this work, we study how to design cost-aware stopping rules, motivated by two primary factors. First, state-of-the-art cost-aware acquisition functions such as the Pandora’s Box Gittins Index (PBGI) (Xie et al., 2024) and log expected improvement per cost (LogEIPC) (Ament et al., 2023) have not yet been studied in the adaptive stopping setting. This is important because—as our experiments in Section 4 will show—for best performance, one should pair different acquisition functions with different stopping rules. Second, while certain stopping rules, such as UCB–LCB (Makarova et al., 2022), are guaranteed to achieve a low simple regret, they are not necessarily guaranteed to do so with low evaluation costs. This is important because—as our experiments will show—UCB–LCB will often incur high evaluation costs, resulting in a high cost-adjusted simple regret.

Our work builds upon the Bayesian-optimal Pandora’s Box decision principle underlying the PBGI acquisition function and extends it to the adaptive stopping setting in correlated Bayesian optimization. Furthermore, we show that an existing stopping rule proposed for the expected improvement (EI) acquisition function in the classical (non-cost-aware) setting (Nguyen et al., 2017) is equivalent to the PBGI stopping rule, which provides a principled extension of that rule to the cost-aware setting. Our stopping rule can therefore naturally be paired with both PBGI and (Log)EI(PC), but it does not automatically extend to acquisition functions based on other design principles (e.g., KG, MES), which would require their own matched stopping rules. Our specific contributions are as follows:

1. *A Novel Cost-Aware Stopping Rule.* We present an adaptive stopping rule derived from Pandora’s box theory, which also naturally extends to the EI design principle, establishing a unified and principled framework applicable to classic and cost-aware Bayesian optimization.
2. *Theoretical Guarantees.* We prove in Theorem 2 that our stopping rule, when paired with the PBGI or LogEIPC acquisition function, satisfies a theoretical upper bound on the expected cost-adjusted simple regret, which constitutes the first theoretical guarantee of this type for any adaptive stopping rule for Bayesian optimization.
3. *Empirical Validation.* We conduct a systematic empirical evaluation across multiple acquisition-function—stopping-rule pairs in cost-aware Bayesian optimization. Our results show that pairing our proposed stopping rule with PBGI or LogEIPC usually matches or outperforms other pairs of acquisition functions and stopping rules.

## 2 BAYESIAN OPTIMIZATION AND ADAPTIVE STOPPING

In black-box optimization, the goal is to find an approximate optimum of an unknown objective function  $f : X \rightarrow \mathbb{R}$  using a limited number of function evaluations at points  $x_1, \dots, x_T \in X$  where  $X$  is the search space and  $T$  is a given search budget, potentially chosen adaptively. The convention measures performance in terms of *expected simple regret* (Garnett, 2023, Sec. 10.1), given by

$$\mathcal{R} = \mathbb{E} \left[ \min_{1 \leq t \leq T} f(x_t) - \inf_{x \in X} f(x) \right] \quad (1)$$

where the expectation is taken over all sources of randomness, including the sequence of points  $x_1, \dots, x_T$  selected by the algorithm. Bayesian optimization approaches this problem by building a probabilistic model of  $f$ —typically a Gaussian process (GP) (Rasmussen & Williams, 2006), conditioned on the observed data points  $(x_t, y_t)_{t=1}^T$ , where  $y_t = f(x_t)$ . For each iteration  $t = 1, \dots, T$ , an acquisition function  $\alpha_t : X \rightarrow \mathbb{R}$  then guides the selection of new samples by carefully balancing the exploration-exploitation tradeoff arising from uncertainty about  $f$ .

### 2.1 COST-AWARE BAYESIAN OPTIMIZATION

*Cost-aware Bayesian optimization* (Lee et al., 2020; Astudillo et al., 2021) extends the above setup to account for the fact that evaluation costs can vary across the search space. For instance, in the hyperparameter tuning example of Section 1, costs can vary according to the time needed to train a

108 machine learning model under a given set of hyperparameters  $x$ . Cost-aware Bayesian optimization  
 109 handles this by introducing a cost function  $c : X \rightarrow \mathbb{R}^+$ , which may be known or unknown ahead.  
 110 The cost function, or observed costs, are then used to construct the acquisition function  $\alpha_t$ .  
 111

112 In this work, we focus primarily on the *cost-per-sample* formulation (Chick & Frazier, 2012; Cashore  
 113 et al., 2016; Xie et al., 2024) of cost-aware Bayesian optimization, which seeks methods with stopping  
 114 time  $\tau$ , not necessarily fixed, that achieve a low *expected cost-adjusted simple regret*

$$115 \quad \mathcal{R}_c = \mathbb{E} \left[ \underbrace{\min_{1 \leq t \leq \tau} f(x_t) - \inf_{x \in X} f(x)}_{\text{simple regret}} + \underbrace{\sum_{t=1}^{\tau} c(x_t)}_{\text{cumulative cost}} \right]. \quad (2)$$

116  
 117  
 118

119 One can also work with the *expected budget-constrained* formulation (Xie et al., 2024), which  
 120 incorporates budget constraints explicitly, and seeks algorithms which achieve a low expected simple  
 121 regret under an expected evaluation budget. Here, performance is evaluated in terms of

$$123 \quad \mathcal{R} = \mathbb{E} \left[ \min_{1 \leq t \leq \tau} f(x_t) - \inf_{x \in X} f(x) \right] \quad \text{where } x_1, \dots, x_{\tau} \text{ satisfy } \mathbb{E} \sum_{t=1}^{\tau} c(x_t) \leq B. \quad (3)$$

124  
 125

The stopping rules we study can be applied in this setting as well: we discuss this in Section 3.1.

127 For both settings, we work with a few acquisition functions—chiefly, *log expected improvement per*  
 128 *cost (LogEIPC)* (Ament et al., 2023) and the *Pandora’s Box Gittins Index (PBGI)* (Xie et al., 2024).  
 129 Given the posterior distribution of  $f$  at iteration  $t$ , LogEIPC is defined as

$$130 \quad \alpha_t^{\text{LogEIPC}}(x) := \log \frac{\text{EI}_{f|x_{1:t}, y_{1:t}}(x; y_{1:t}^*)}{c(x)}, \quad (4)$$

131  
 132

133 i.e., the logarithm of the expected improvement divided by the cost; and PBGI is defined as

$$134 \quad \alpha_t^{\text{PBGI}}(x) := \begin{cases} g & \text{where } g \text{ solves } \text{EI}_{f|x_{1:t}, y_{1:t}}(x; g) = c(x), & x \notin \{x_1, \dots, x_t\} \\ f(x), & & x \in \{x_1, \dots, x_t\} \end{cases} \quad (5)$$

135  
 136

137 where the value  $g$  is the threshold at which the expected improvement equals the cost<sup>1</sup>,  $y_{1:t}^* =$   
 138  $\min_{1 \leq s \leq t} y_s$  is the best value observed in the first  $t$  iterations, and  $\text{EI}_{\psi}(x; y) = \mathbb{E}[\max(y - \psi(x), 0)]$   
 139 is the expected improvement at point  $x$  with respect to some random function  $\psi : X \rightarrow \mathbb{R}$  and a  
 140 baseline value  $y$ . We also consider classical cost-unaware acquisition functions—*lower confidence*  
 141 *bound (LCB)* and *Thompson sampling (TS)*; see Garnett (2023) for details.

## 142 2.2 ADAPTIVE STOPPING RULES

144 To the best of our knowledge, stopping rules for Bayesian optimization typically do not incorporate  
 145 cost explicitly into the stopping criterion. We broadly categorize existing methods as follows:

147 *Criteria based on convergence or significance of improvement.* This includes empirical convergence,  
 148 namely stopping when the best value remains unchanged for a fixed number of iterations, or the  
 149 *global stopping strategy (GSS)* (Bakshy et al., 2018), which stops when the improvement is no longer  
 150 statistically significant relative to the inter-quartile range (i.e., the range between the 25th percentile  
 151 and the 75th percentile) of prior observations. In the multi-fidelity setting, Foumani & Bostanabad  
 152 (2025) proposed stopping when the high-fidelity surrogate’s estimated optimum has stabilized over a  
 153 window of iterations, which is related to cost-awareness but differs from our setting with explicitly  
 154 varying evaluation costs.

155 *Acquisition-based criteria.* This includes stopping rules built from acquisition functions such as  
 156 the *probability of improvement (PI)* (Lorenz et al., 2015), *expected improvement (EI)* (Locatelli,  
 157 1997; Nguyen et al., 2017; Ishibashi et al., 2023), and *knowledge gradient (KG)* (Frazier & Powell,  
 158 2008). These approaches typically stop when the acquisition value falls below a fixed threshold—a  
 159 predetermined constant, median of the initial acquisition values, or the cost of sampling—but typically  
 160 assume uniform costs and do not adapt to evaluation costs which can vary across the search space.

161 <sup>1</sup>For an evaluated point  $x$ , we set  $g = f(x)$  since the posterior at  $x$  collapses to a point mass at the observed  
 162 value  $f(x)$  and its evaluation cost can be treated as 0.

162 *Regret-based criteria.* This includes stopping rules based on confidence bounds such as *UCB-LCB*  
 163 (Makarova et al., 2022) and the *gap of expected minimum simple regrets* (Ishibashi et al., 2023).  
 164 These stop when certain estimated regret bounds fall below a preset or data-driven threshold. The  
 165 related *probabilistic regret bound (PRB)* stopping rule (Wilson, 2024) stops when estimated simple  
 166 regret is below a small threshold  $\epsilon$  with confidence  $1 - \delta$ .

167 In settings beyond Bayesian optimization, Chick & Frazier (2012) have proposed a cost-aware  
 168 stopping rules for finite-domain sequential sampling problems with independent values. Although  
 169 this formulation allows for varying costs, it does not extend to general Bayesian optimization settings  
 170 which use correlated GP models.  
 171

### 172 3 A STOPPING RULE BASED ON THE PANDORA'S BOX GITTINS INDEX

173 In this work, we propose a new stopping rule tailored for two state-of-the-art acquisition functions  
 174 used in cost-aware Bayesian optimization: LogEIPC and PBGI, introduced in Section 2. As discussed  
 175 by Xie et al. (2024), these acquisition functions are closely connected, arising from two different  
 176 approximations of the intractable dynamic program which defines the Bayesian-optimal policy for  
 177 cost-aware Bayesian optimization. We now show that this connection can be used to obtain a  
 178 principled stopping criterion to be paired with both acquisition functions.  
 179

180 **A stopping rule for PBGI.** To derive a stopping rule for PBGI, consider first the Pandora's Box  
 181 problem, from which it is derived. Pandora's Box can be seen as a special case of cost-per-sample  
 182 Bayesian optimization, as introduced in Section 2, where  $X = \{1, \dots, N\}$  is a discrete space  
 183 and  $f$  is assumed uncorrelated. In this setting, the observed values do not affect the posterior  
 184 distribution—meaning, we have  $f(x') \mid x_{1:t}, y_{1:t} = f(x')$  at all unobserved points  $x'$ —and thus the  
 185 acquisition function value at point  $x$  is time-invariant and can be written simply as  $\alpha^{\text{PBGI}}(x)$ , where  
 186  $\text{EI}_f(x; \alpha^{\text{PBGI}}(x)) = c(x)$ . Following Weitzman (1979), one can show using a Gittins index argument  
 187 that selecting  $x_t$  to minimize  $\alpha^{\text{PBGI}}$  is Bayesian-optimal under minimization—the algorithm which  
 188 does so achieves the smallest expected cost-adjusted simple regret, among all adaptive algorithms.  
 189

190 One critical detail applied in the optimality argument of Weitzman (1979) is that the policy defined  
 191 by  $\alpha^{\text{PBGI}}$  is *not* Bayesian-optimal for any fixed deterministic  $T$ . Instead, it is optimal only when the  
 192 stopping time  $T$  is chosen according to the condition

$$193 \min_{x \in X \setminus \{x_1, \dots, x_t\}} \alpha^{\text{PBGI}}(x) \geq y_{1:t}^* \quad (6)$$

195 where  $\geq$  can be replaced by  $>$ <sup>2</sup>, and as before,  $y_{1:t}^*$  is the best value observed so far.

196 In the correlated setting we study, Xie et al. (2024) extend  $\alpha^{\text{PBGI}}$  to define an acquisition function by  
 197 recomputing it at each time step  $t$  based on the posterior mean and variance, which defines  $\alpha_t^{\text{PBGI}}$  as  
 198 in Equation (5). In order to also extend the associated stopping rule, a subtle design choice arises:  
 199 should we use  $\alpha_{t-1}^{\text{PBGI}}$  (before posterior update) or  $\alpha_t^{\text{PBGI}}$  (after posterior update) in Equation (6)?  
 200 While prior theoretical work (Gergatsouli & Tzamos, 2023) adopts the former choice, we instead  
 201 propose the latter, for two main reasons.

202 First, we argue it more faithfully reflects the intuition behind Weitzman's original stopping rule.  
 203 In the independent setting,  $\alpha^{\text{PBGI}}(x)$  represents a kind of *fair value* for point  $x$  (Kleinberg et al.,  
 204 2016). For an evaluated point  $x \in \{x_1, \dots, x_t\}$ , this is simply the observed function value. For an  
 205 unevaluated point  $x \notin \{x_1, \dots, x_t\}$ , the fair value reflects uncertainty in  $f(x)$  and the cost  $c(x)$ . The  
 206 stopping rule Equation (6) then says to *stop when the best fair value is among the already-evaluated*  
 207 *points*—namely, when no point provides positive expected gain relative to its cost if evaluated in the  
 208 next round, conditioned on current observations. In the correlated setting, the fair value naturally  
 209 extends to  $\alpha_t^{\text{PBGI}}$ , because this incorporates all known information at a given time. Second, we show  
 210 in Appendix D.2 that using  $\alpha_t^{\text{PBGI}}$  yields tangible empirical gains in cost-adjusted regret.

211 **Connection with LogEIPC.** The above reasoning may at first seem to be fundamentally tied to  
 212 the Pandora's Box problem and its Gittins-index-theoretic properties. We now show that it admits a

213  
 214 <sup>2</sup>Following Xie et al. (2024, Appendix B), optimality holds under any tie-breaking rule in the cost-per-sample  
 215 setting, but only under a carefully-chosen stochastic tie-breaking rule in the expected budget-constrained setting.  
 For simplicity, we use the stopping-as-early-as-possible tie-breaking rule throughout this paper.

216 second interpretation in terms of log expected improvement per cost, which arises from a completely  
 217 different one-time-step approximation to the Bayesian-optimal dynamic program for cost-aware  
 218 Bayesian optimization in the general correlated setting.

219 To show this, we start with definitions above and apply a sequence of transformations. Recall that for  
 220 any unevaluated point  $x \notin \{x_1, \dots, x_t\}$ ,  $\alpha_t^{\text{PBGI}}(x)$  is defined in Equation (5) to be the solution to  
 221

$$\text{EI}_{f|x_{1:t}, y_{1:t}}(x; \alpha_t^{\text{PBGI}}(x)) = c(x) \quad (7)$$

222 and since  $\text{EI}_\psi(x; y)$  is strictly increasing in  $y$ , any inequality involving  $\alpha_t^{\text{PBGI}}(x; c)$  can be lifted  
 223 through the EI function without changing its direction, which means

$$\alpha_t^{\text{PBGI}}(x) \geq y_{1:t}^* \quad \text{holds if and only if} \quad \text{EI}_{f|x_{1:t}, y_{1:t}}(x; y_{1:t}^*) \leq c(x). \quad (8)$$

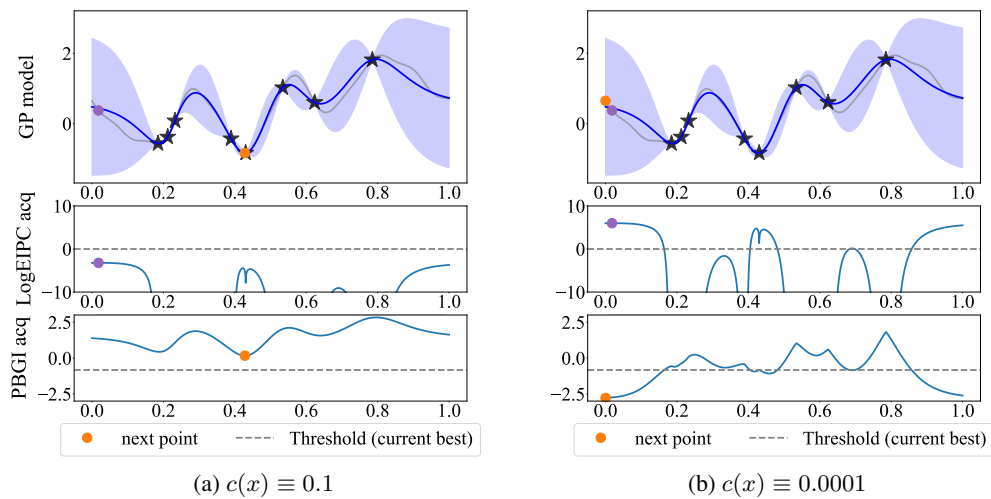
224 This implies that the PBGI stopping rule from Equation (6) is equivalent to stopping when  
 225

$$\text{EI}_{f|x_{1:t}, y_{1:t}}(x; y_{1:t}^*) \leq c(x) \quad \text{for all } x \in X \setminus \{x_1, \dots, x_t\}. \quad (9)$$

226 meaning *stop when no point's expected improvement is worth its evaluation cost*. Rearranging the  
 227 inequality and taking logs, we can rewrite this condition using the LogEIPC acquisition function<sup>3</sup> :

$$\max_{x \in X \setminus \{x_1, \dots, x_t\}} \alpha_t^{\text{LogEIPC}}(x; y_{1:t}^*) \leq 0. \quad (10)$$

228 We call the stopping rule given by the equivalent conditions (Equations (6), (9) and (10)) the  
 229 *PBGI/LogEIPC stopping rule*. Figure 1 gives an illustration of how the rule behaves in a simple  
 230 setting, demonstrating that it is more conservative—preferring to stop earlier—when the cost is high.



229 Figure 1: Illustration of the PBGI/LogEIPC stopping rule under a uniform-cost setting. When the  
 230 cost-per-sample is large ( $c(x) \equiv 0.1$ ), the maximum LogEIPC acquisition value falls below the  
 231 threshold 0.0 and the minimum PBGI acquisition value exceeds the current best observed value,  
 232 indicating stopping; when the cost-per-sample is small ( $c(x) \equiv 0.0001$ ), the maximum LogEIPC  
 233 acquisition value remains above the threshold 0.0 and the minimum PBGI acquisition value is smaller  
 234 than the current best observed value, indicating no stopping.

### 235 3.1 THEORETICAL GUARANTEES ON COST-ADJUSTED SIMPLE REGRET

236 The connection between PBGI and LogEIPC in fact goes beyond a shared stopping rule. In Lemma 1,  
 237 we prove that when paired with this stopping rule, both acquisition functions guarantee that at each  
 238 iteration before stopping, the expected improvement at the selected point is at least its evaluation cost.

239 <sup>3</sup>Excluding evaluated points is not theoretically required but often beneficial in practice, as numerical stability  
 240 adjustments can cause their expected improvement to remain positive.

270 **Lemma 1.** Let  $X$  be compact, and let  $f : X \rightarrow \mathbb{R}$  be a random function with *prior mean*  $\mu(\cdot)$ .  
 271 Consider a Bayesian optimization algorithm that begins at some initial point  $x_1 \in X$  with cost  
 272  $C = c(x_1)$ , acquires subsequent points using either the PBGI or LogEIPC acquisition function, and  
 273 terminates according to the PBGI/LogEIPC stopping rule. Let  $\tau = \min_{t \geq 1} \{\sup_{x \in X} \alpha_t^{\text{LogEIPC}}(x) <$   
 274  $0\}$  be the algorithm's stopping time, and denote the posterior expected improvement function by  
 275  $\alpha_t^{\text{EI}}(x) = \text{EI}_{f|x_{1:t}, y_{1:t}}(x; y_{1:t}^*)$ . Then, for all  $t < \tau$ ,  $\alpha_t^{\text{EI}}(x_{t+1}) \geq c(x_{t+1})$ .  
 276

277 As a consequence of this claim, we show in Theorem 2 that the PBGI/LogEIPC stopping rule, when  
 278 paired with PBGI or LogEIPC, achieves cost-adjusted simple regret no worse than stopping immedi-  
 279 ately after the initial evaluation. Although this may sound trivial, many acquisition function-stopping  
 280 rule pairs fail to satisfy this *no-worse-than-immediate* property in practice (see Figures 2 and 3),  
 281 largely because most stopping rules are designed with simple regret alone in mind and do not explic-  
 282 itly account for evaluation costs. To our knowledge, this is the first formal guarantee on cost-adjusted  
 283 simple regret for Bayesian optimization, generalizing beyond simpler settings such as Pandora's Box,  
 284 which assumes independent and discrete evaluations. All proofs in this section are in Appendix B.  
 285

286 **Theorem 2.** Consider the setting and algorithm specified in Lemma 1. Let  $U := \mu(x_1) -$   
 $\mathbb{E}[\min_{x \in X} f(x)] < \infty$ , then the algorithm's expected cost-adjusted simple regret is bounded by

$$287 \mathbb{E} \left[ y_{1:\tau}^* - \min_{x \in X} f(x) + \sum_{t=1}^{\tau} c(x_t) \right] \leq \mathbb{E} \left[ \underbrace{y_1 - \min_{x \in X} f(x) + c(x_1)}_{\text{cost-adjusted regret of immediate stopping}} \right] = U + C. \quad (11)$$

290 This result yields a bound on expected cumulative cost and, under the natural assumption that practical  
 291 evaluations have a positive minimum cost, a high-probability finite-time termination guarantee.

292 **Corollary 3.** Consider the setting and algorithm specified in Lemma 1. Then the expected cumulative  
 293 cost of the algorithm is bounded by  $\mathbb{E}[\sum_{t=1}^{\tau} c(x_t)] \leq U + C$ . Further, if evaluation costs are  
 294 uniformly bounded below by a constant  $c_0 > 0$ , i.e.,  $c(x) \geq c_0, \forall x \in X$ , then for any  $\delta \in (0, 1)$ , the  
 295 algorithm terminates in at most  $\frac{U+C}{\delta \cdot c_0}$  iterations with probability  $1 - \delta$ .  
 296

### 298 3.1.1 IMPLICATION IN THE BUDGET-CONSTRAINED SETTING

300 We first note that in the discrete Pandora's Box setting, under an expected budget constraint  $B$ ,  
 301 minimizing  $\alpha_t^{\text{PBGI}}(x)$  is Bayesian-optimal: it achieves the lowest *expected simple regret*, among all  
 302 algorithms satisfying  $\mathbb{E}[\sum_{t=1}^{\tau} c(x_t)] \leq B$ , and the cost function used in defining  $\alpha_t^{\text{PBGI}}(x)$  is  $\lambda c(x)$   
 303 for some cost-scaling factor  $\lambda$  which depends on  $B$  (Xie et al., 2024, Theorem 2).

304 This result, at first, appear to be completely Pandora's-Box-theoretic: it requires  $X$  to be discrete  
 305 and  $f$  to be independent. In the more general correlated setting of cost-aware Bayesian optimization,  
 306 however, Bayesian optimality of PBGI may no longer hold, and the relationship between  $B$  and the  
 307 choice of  $\lambda$  is not immediately clear. Theorem 2 helps bridge this gap: it provides an upper bound on  
 308 the expected cumulative cost up to the stopping time, which in turn yields the following principled  
 309 choice of  $\lambda$  that ensures compliance with the budget constraint.

310 **Corollary 4.** Consider the setting, algorithm, and notation specified in Lemma 1 and Theorem 2, but  
 311 with costs rescaled by a factor  $\lambda > 0$ : both the acquisition values and the stopping conditions are  
 312 computed using  $\lambda c(\cdot)$ . If the cost-scaling factor is set to  $\lambda = \frac{U}{B-C}$ , then the algorithm's expected  
 313 cumulative unscaled cost satisfies  $\mathbb{E}[\sum_{t=1}^{\tau} c(x_t)] \leq B$ .

314 If this choice of  $\lambda$  proves overly conservative—leading to underspending within the budget—it can  
 315 be paired with the PBGI-D variant of Xie et al. (2024), which starts with  $\lambda = \lambda_0$  and halves it each  
 316 time stopping is triggered. Choosing  $\lambda_0 = U/(B - C)$  aligns the initial fixed- $\lambda$  phase with the  
 317 budget in expectation, while ensuring that the adaptive decay is activated as designed. In Figure 10 in  
 318 Appendix D, we show PBGI-D with this choice of  $\lambda_0$  is competitive.  
 319

## 320 3.2 PRACTICAL IMPLEMENTATION CONSIDERATIONS FOR PBGI/LOGEIPC STOPPING RULE

321 **Expressing objective and cost in common units.** Evaluation costs are often measured in different  
 322 units than the objective, such as time versus accuracy. To compare them directly, we rescale costs  
 323 by a constant  $\lambda > 0$ , the conversion rate between cost and objective improvement. For instance, if

324 one is willing to spend 1000 seconds to reduce test error by 0.01, then  $\lambda = 10^{-5}$ . Importantly, in the  
 325 cost-per-sample setting we mainly study,  $\lambda$  is set by the problem provider rather than tuned by the  
 326 user, whereas the budgeted setting without a natural unit conversion is discussed in Section 3.1.1.  
 327

328 **Unknown costs.** In practice, evaluation costs are often not known in advance. They can be  
 329 modeled either (i) deterministically, using domain knowledge (e.g., proportional to model size in  
 330 hyperparameter tuning), or (ii) stochastically, via a GP over log costs. In Section 4, we present  
 331 empirical benchmark results under both modeling approaches. For the stochastic approach, we  
 332 follow Astudillo et al. (2021, Proposition 2) to model  $\ln c(x)$  as a GP with posterior mean  $\mu_{\ln c}$  and  
 333 variance  $\sigma_{\ln c}^2$ . To compute LogEIPC or PBGI, as well as their related stopping rules (including  
 334 prior acquisition-based ones and ours), we replace  $c(x)$  in Equations (4), (5) and (9) with  $\mathbb{E}[c(x)] =$   
 335  $\exp(\mu_{\ln c}(x) + (\sigma_{\ln c}(x))^2/2)$ . See Appendix D.3 for further discussion.

336 **Preventing spurious stops.** Although our stopping rule has theoretical guarantees, in practice,  
 337 it—like other adaptive stopping rules—can still suffer from spurious stops caused by two main  
 338 sources. First, early in the optimization process, the GP model parameters often fluctuate significantly  
 339 as new data points are collected, causing unstable stopping signals. To mitigate this, we enforce  
 340 a stabilization period consisting of the first several evaluations, during which we do not allow any  
 341 stopping rule to trigger. Second, imperfect optimization of the acquisition function—which is  
 342 especially common in higher-dimensional search spaces—can lead to misleading stopping signals. To  
 343 handle this, we use a *debounce* strategy, requiring the stopping rule to consistently indicate stopping  
 344 over several consecutive iterations before stopping optimization. [See Figure 4 for an illustration.](#)  
 345

## 346 4 EXPERIMENTS

347 To evaluate our proposed PBGI/LogEIPC stopping rule, we design three complementary sets of  
 348 experiments that progressively test its performance. First, we consider an idealized, low-dimensional  
 349 Bayesian regret setting in which the GP model exactly matches the true objective. This controlled  
 350 environment allows us to isolate the effect of different stopping rules without interference from  
 351 modeling or optimization errors. Then, we move to a higher-dimensional Bayesian regret setting  
 352 where each acquisition-function minimization must be approximated via a numerical optimizer.  
 353 Finally, we test in practical scenarios with potential objective model mismatch, using the LCBench  
 354 hyperparameter tuning benchmark and the NATS neural architecture size search benchmark. In each  
 355 case, we compare pairs of acquisition functions and stopping rules, which we describe next.  
 356

357 **Acquisition functions.** We consider four common acquisition functions that were discussed in  
 358 Section 2: LogEIPC, PBGI, LCB, and TS—chosen for their competitive performance, computational  
 359 efficiency, and close connections to existing stopping rules.  
 360

361 **Baselines.** We compare the proposed PBGI/LogEIPC stopping rule against several stopping rules  
 362 from prior work: *UCB–LCB* (Makarova et al., 2022), *LogEIPC-med* (Ishibashi et al., 2023), *SRGap-  
 363 med* (Ishibashi et al., 2023), and *PRB* (Wilson, 2024). We also include two simple heuristics  
 364 used in practice: *Convergence* and *GSS*. *UCB–LCB* stops once the gap between upper and lower  
 365 confidence bounds falls below a configurable threshold  $\theta$ . *LogEIPC-med* stops when the log expected  
 366 improvement per cost drops beneath  $\log(\eta)$  plus the median of its initial  $I$  values. *SRGap-med*  
 367 stops when the gap of the expected minimum simple regret falls below  $\chi$  times the median of its  
 368 initial  $I$  values. *PRB* triggers once a probabilistic regret bound satisfies the regret tolerance  $\epsilon$  and  
 369 confidence  $\delta$  parameters. *Convergence* stops as soon as the best observed value remains unchanged  
 370 for  $w$  iterations. *GSS* stops if the recent improvement is less than  $\phi \times \text{IQR}$  over the past  $w$  trials  
 371 where IQR denotes the inter-quartile range of current observations. Finally, we include two reference  
 372 baselines: *Immediate*, which stops right after the initial evaluation (see Section 3.1), and *Hindsight*,  
 373 which, for each trial, selects the stopping time that yields the lowest cost-adjusted simple regret in  
 374 hindsight, thus providing a lower bound on achievable performance.

375 In our experiments, unless specified otherwise, we follow parameter values recommended in the  
 376 literature, and set  $\theta = 0.01$ ,  $\eta = 0.01$ ,  $\chi = 0.01$ ,  $I = 20$ ,  $\epsilon = 0.1$  for Bayesian regret experiments,  
 377  $\epsilon = 0.5\%$  of the best test error for empirical experiments,  $\delta = 0.05$ ,  $w = 5$ , and  $\phi = 0.01$ . Each  
 378 experiment is repeated with 50 random seeds to assess variability, and we report the mean with error

378 bars (2 times the standard error) for each stopping rule. Each trial, in the sense of a run with a distinct  
 379 random seed, is capped at a fixed number of iterations; if a stopping rule is not triggered within this  
 380 limit, the stopping time is set to the cap. Details are provided in Appendix C.  
 381

382 **4.1 BAYESIAN REGRET**  
 383

384 We first evaluate our PBGI/LogEIPC stopping rule on random functions sampled from prior. Specifi-  
 385 cally, objective functions are sampled from Gaussian processes with Matérn 5/2 kernels with length  
 386 scale 0.1, defined over spaces of dimension  $d = 1$  and  $d = 8$ . We consider a variety of evaluation cost  
 387 function types, including uniform costs, linearly increasing costs in terms of parameter magnitude,  
 388 and periodic costs that vary non-monotonically over the domain.  
 389

390 In the 1-dimensional experiments, we perform an exhaustive grid search over  $[0, 1]$  to isolate the effect  
 391 of stopping behavior from numerical optimization. In the 8-dimensional setting, due to instability  
 392 from higher dimensionality, we apply moving average with a window size of 20 when computing the  
 393 PBGI/LogEIPC stopping condition. See Figure 4 in Appendix C for an illustration. More details on  
 394 our experiment setup, and computational considerations are provided in Appendices C and D.  
 395

396 Figure 2 shows a comparison of cost-adjusted regret for acquisition function and stopping rule  
 397 pairings under different cost-scaling factors  $\lambda$  in the 1-dimensional setting and under different cost  
 398 regimes (uniform, linear, periodic) in 8-dimensional setting.  
 399

400 In the 1-dimensional setting, the Bayesian optimization problem is relatively straightforward and  
 401 all acquisition functions attain nearly identical hindsight optima, independent of cost scale or cost  
 402 type. From the plot, our PBGI/LogEIPC stopping rule pairing with LogEIPC or PBGI acquisition  
 403 function delivers competitive performance for each  $\lambda$ , and is particularly strong in handling high-cost  
 404 scenarios—those with large  $\lambda$ .  
 405

406 In the 8-dimensional experiments, however, clear gaps emerge: Under uniform and linear costs,  
 407 LogEIPC, PBGI, and LCB perform similarly and substantially outperform TS, while in the periodic  
 408 case, LogEIPC and PBGI outperform LCB and TS. In every cost regime, combining our stopping rule  
 409 with the LogEIPC, PBGI, or LCB acquisition function yields cost-adjusted regret nearly matching  
 410 the hindsight optimal. This shows our PBGI/LogEIPC stopping rule to be relatively robust against  
 411 challenges in acquisition function optimization. Further discussions of our experiments across all  
 412 cost types and cost-scaling factors can be found in Appendix D.  
 413

414 **4.2 EMPIRICAL AUTOMATED MACHINE LEARNING BENCHMARKS**  
 415

416 We then evaluate on two empirical benchmarks based on use cases from hyperparameter optimization  
 417 and neural architecture search: LC-Bench (Zimmer et al., 2021) and NATS-Bench (Dong et al., 2021).  
 418

419 LC-Bench provides training data of 2,000 hyperparameter configurations evaluated on 35 OpenML  
 420 Vanschoren et al. (2014) datasets. In the *unknown-cost* experiments, the cost is the full (200-epoch)  
 421 training time. For the known-cost setting, we observe that training time to scale approximately  
 422 linearly with the number of model parameters. Based on a linear regression fit (see Appendix C),  
 423 we adopt  $\alpha p$  as a proxy of training time, where  $p$  is the number of model parameters and  $\alpha$  is a  
 424 dataset-specific coefficient estimated from the regression.  
 425

426 NATS-Bench provides a search space of 32,768 neural architectures varying in channel sizes across  
 427 layers, evaluated on three datasets. As in LC-Bench, for the known-cost experiments, we approximate  
 428 the full runtime (training + validation time) at 90 epochs using  $\alpha F + \beta$ , where  $F$  is the number of  
 429 floating point operations; see Appendix C for details.  
 430

431 We report the mean and error bars (2 times standard error) of the *cost-adjusted simple regret*, where  
 432 we consider the evaluation costs to be some representative cost-scaling factor  $\lambda$  (see Section 3.2)  
 433 multiplied with cumulative runtime. Simple regret is computed as the difference between (a) test  
 434 error of the configuration with best validation error at the stopping time and (b) the best test error  
 435 over all configurations. We present the results using proxy runtime here, and defer to Appendix D the  
 436 additional results under (i) the *cost model mismatch* scenario (proxy runtime used during Bayesian  
 437 optimization but actual runtime used for final performance evaluation), and (ii) the *unknown-cost*  
 438 scenario (actual runtime used during Bayesian optimization).  
 439

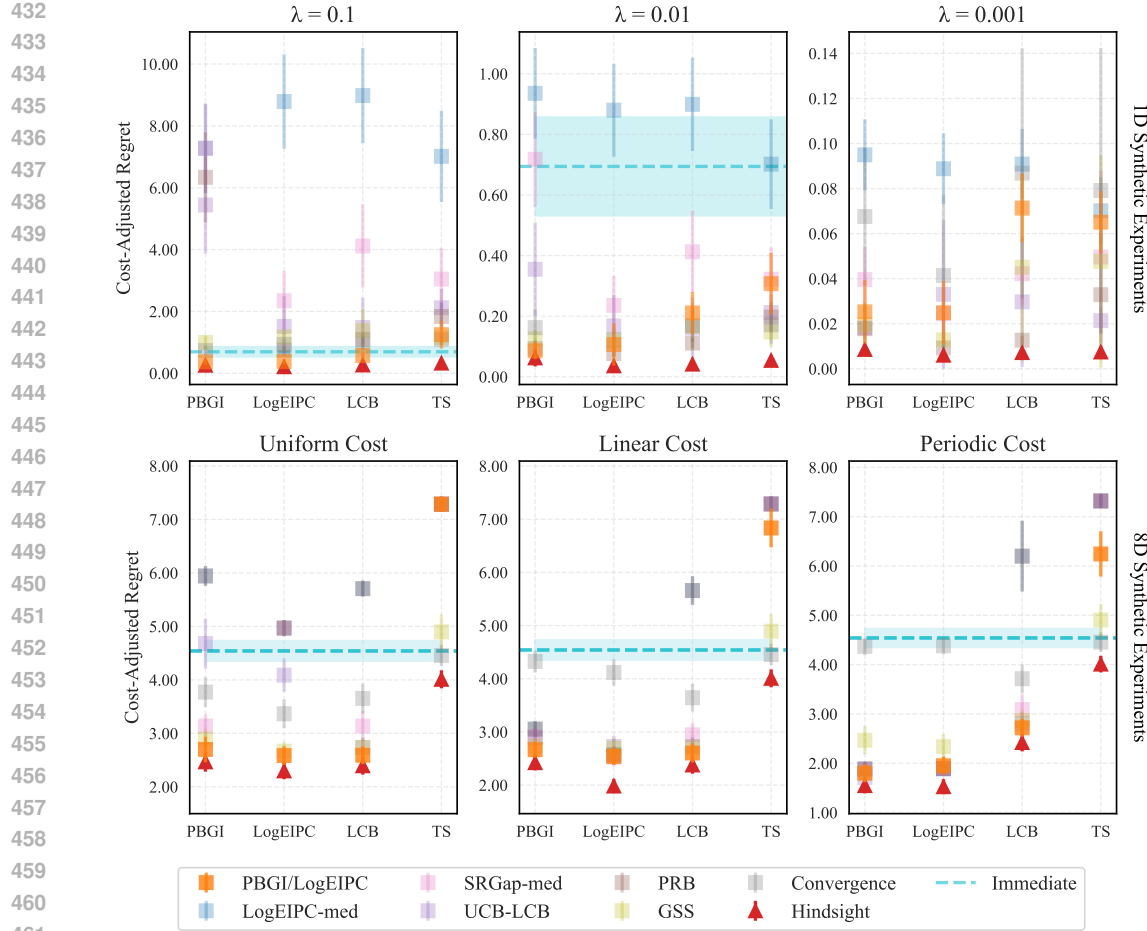


Figure 2: Cost-adjusted simple regret across acquisition-stopping rule pairs in 1D and 8D Bayesian regret setting. In 1D, objective functions are sampled from a GP with a Matérn-5/2 kernel and a linear cost function scaled by  $\lambda = 0.1, 0.01, 0.001$ . The Immediate baseline is omitted at  $\lambda = 0.001$  due to its much higher regret (mean 0.6942, error bar [0.5314, 0.8570]). In 8D, objective functions are also drawn from a GP with a Matérn-5/2 kernel, using three cost functions scaled by  $\lambda = 0.01$ .

Figure 3 presents performance of acquisition function–stopping rule pairs on LCBench and NATS-Bench. For LCBench, we report min–max normalized cost-adjusted simple regret (see definition in Appendix D) aggregated across 35 datasets in Figure 3 evaluated under three representative<sup>4</sup> cost-scaling values. For NATS-Bench, we report cost-adjusted simple regret under  $\lambda = 10^{-5}$ , with additional results under two other cost-scaling factors shown in Figures 14 to 16 in Appendix D.

Per-dataset LCBench results are provided in Figures 19 to 21 in the appendix. Across these 35 tasks, around 75% of them show our PBGI/LogEIPC stopping rule performing competitively when paired with either PBGI or LogEIPC. The remaining outliers are mostly (aside from two exceptions) very small datasets with <10000 instances that might lead to severe model misspecification.

Additional results under the cost model mismatch setting and the unknown-cost setting are provided in Figures 17 and 18 in Appendix D, along with comparisons between our adaptive stopping rule and fixed-iteration baselines. Overall, our PBGI/LogEIPC stopping rule consistently performs strongly in terms of cost-adjusted simple regret, when paired with either PBGI or LogEIPC. We also report, in Table 1 of Appendix D, how often each stopping rule fails to trigger within the 200-iteration cap: baselines such as SRGap-med and UCB-LCB often fail to stop early—particularly on NATS-Bench—whereas our stopping rule reliably stops before the cap.

<sup>4</sup>These  $\lambda$  values are chosen to avoid degenerate cases—neither so large that the policy stops after only a few evaluations (e.g.,  $\lambda = 10^{-4}$  on NATS-Bench, see Figure 17) nor so small that evaluations are effectively free.

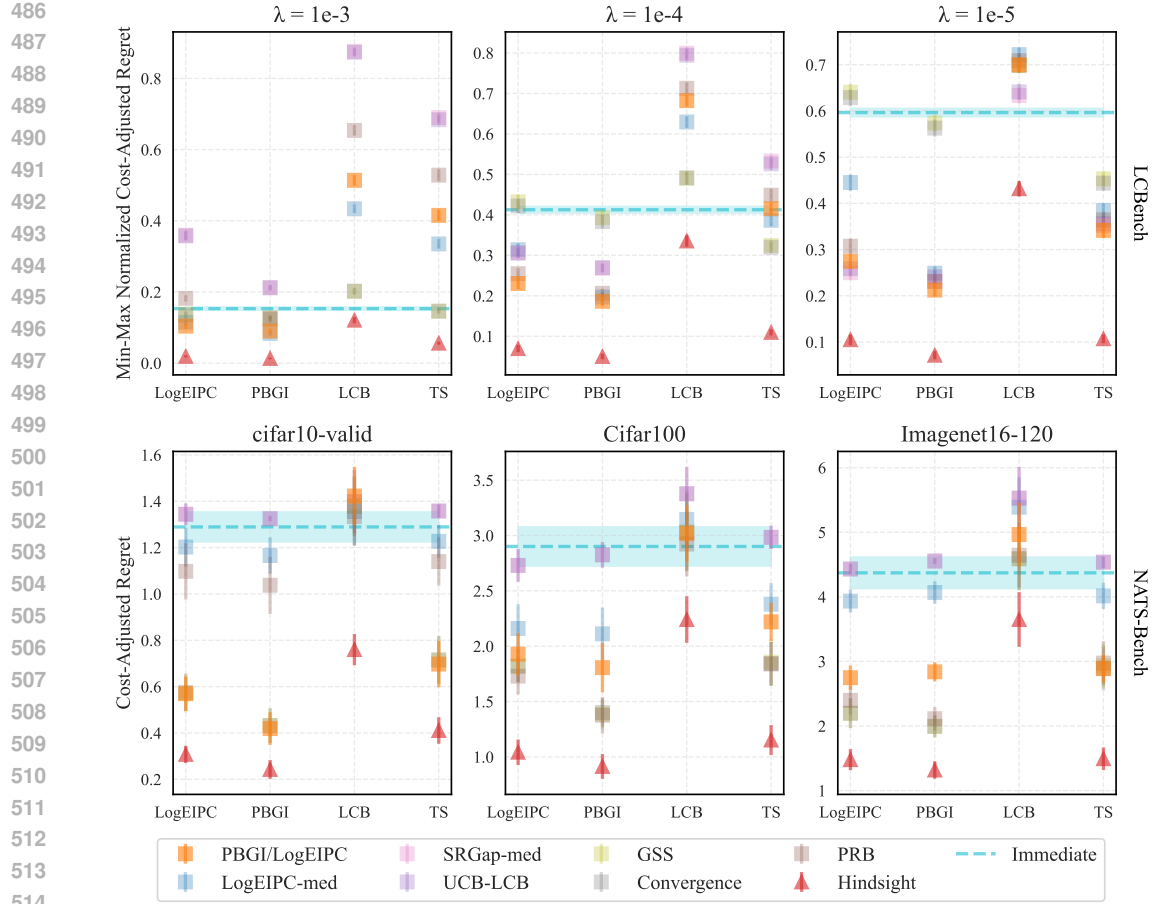


Figure 3: Cost-adjusted simple regret across acquisition function-stopping rule pairs on LCBench and NATS-Bench. The objective is to minimize validation error on classification tasks, with scaled proxy runtime as evaluation cost, scaled by representative values of  $\lambda$  ( $10^{-3}, 10^{-4}, 10^{-5}$  for LCBench and  $10^{-5}$  for NATS-Bench). For LCBench, results are aggregated across 35 datasets using min–max normalization. Our PBGI/LogEIPC stopping rule, when paired with either LogEIPC or PBGI, typically ranks among the top 3 pairs and closely approaches the hindsight optimal on LCBench and on cifar10-valid in NATS-Bench, but slightly worse on the other two NATS datasets.

As we transition from model match to model mismatch, where the true objective function does not align perfectly with the GP prior, we find that our stopping rule, when paired with the PBGI acquisition function, continues to deliver performance close to the hindsight optimal, except on two NATS datasets likely affected by severe mismatch. In contrast, pairing with the LogEIPC acquisition function is less competitive. This degradation appears to stem from the relative advantage of PBGI over LogEIPC in higher dimensions or misspecified settings: as shown in Figure 10 in Appendix D, PBGI maintains stronger performance under misspecification, thus contributing to the improved overall cost-adjusted regret. Thus, while our stopping rule is broadly robust, the choice of acquisition function remains an important consideration when facing objective model mismatch.

## 5 CONCLUSION

We develop the *PBGI/LogEIPC stopping rule* for Bayesian optimization with varying evaluation costs. Paired with either the PBGI or LogEIPC acquisition function, it (a) satisfies a theoretical guarantee bounding the expected cost-adjusted simple regret (Section 3.1), and (b) shows strong empirical performance in terms of cost-adjusted simple regret (Section 4). We believe our framework can be extended to settings involving noisy, multi-fidelity or batched evaluations, as well as alternative objective formulations—for instance, applying a sigmoid transformation to test error rather than a linear one, to reflect real-world user preferences that shift sharply once error falls below a threshold.

540 REFERENCES  
541

542 Sebastian Ament, Samuel Daulton, David Eriksson, Maximilian Balandat, and Eytan Bakshy. Unex-  
543 pected improvements to expected improvement for bayesian optimization. *Advances in Neural*  
544 *Information Processing Systems*, 36:20577–20612, 2023.

545 Raul Astudillo, Daniel Jiang, Maximilian Balandat, Eytan Bakshy, and Peter I Frazier. Multi-step  
546 budgeted bayesian optimization with unknown evaluation costs. In *Advances in Neural Information*  
547 *Processing Systems*, 2021.

548 Eytan Bakshy, Lili Dworkin, Brian Karrer, Konstantin Kashin, Benjamin Letham, Ashwin Murthy,  
549 and Shaun Singh. Ae: A domain-agnostic platform for adaptive experimentation. In *Conference*  
550 *on neural information processing systems*, pp. 1–8, 2018.

552 Maximilian Balandat, Brian Karrer, Daniel Jiang, Samuel Daulton, Ben Letham, Andrew G Wil-  
553 son, and Eytan Bakshy. Botorch: A framework for efficient monte-carlo bayesian optimization.  
554 *Advances in neural information processing systems*, 33:21524–21538, 2020.

555 J Massey Cashore, Lemuel Kumarga, and Peter I Frazier. Multi-step bayesian optimization for  
556 one-dimensional feasibility determination. *arXiv preprint arXiv:1607.03195*, 2016.

558 Stephen E Chick and Peter Frazier. Sequential sampling with economics of selection procedures.  
559 *Management Science*, 58(3):550–569, 2012.

561 Xuanyi Dong, Lu Liu, Katarzyna Musial, and Bogdan Gabrys. Nats-bench: Benchmarking nas  
562 algorithms for architecture topology and size. *IEEE transactions on pattern analysis and machine*  
563 *intelligence*, 44(7):3634–3646, 2021.

564 Zahra Zanjani Foumani and Ramin Bostanabad. Constrained multi-fidelity bayesian optimization  
565 with automatic stop condition. *CoRR*, abs/2503.01126, 2025. doi: 10.48550/ARXIV.2503.01126.  
566 URL [HTTPS://DOI.ORG/10.48550/ARXIV.2503.01126](https://doi.org/10.48550/ARXIV.2503.01126).

568 Peter Frazier and Warren B Powell. The knowledge-gradient stopping rule for ranking and selection.  
569 In *2008 Winter Simulation Conference*, pp. 305–312. IEEE, 2008.

570 Roman Garnett. *Bayesian optimization*. Cambridge University Press, 2023.

572 Evangelia Gergatsouli and Christos Tzamos. Weitzman’s rule for pandora’s box with correlations.  
573 *Advances in Neural Information Processing Systems*, 36:12644–12664, 2023.

575 Shouri Hu, Haowei Wang, Zhongxiang Dai, Bryan Kian Hsiang Low, and Szu Hui Ng. Adjusted  
576 expected improvement for cumulative regret minimization in noisy bayesian optimization. *Journal*  
577 *of Machine Learning Research*, 26(46):1–33, 2025.

578 Hideaki Ishibashi, Masayuki Karasuyama, Ichiro Takeuchi, and Hideitsu Hino. A stopping criterion  
579 for bayesian optimization by the gap of expected minimum simple regrets. In *International*  
580 *Conference on Artificial Intelligence and Statistics*, pp. 6463–6497. PMLR, 2023.

582 Robert Kleinberg, Bo Waggoner, and E Glen Weyl. Descending price optimally coordinates search.  
583 *arXiv preprint arXiv:1603.07682*, 2016.

584 Eric Hans Lee, Valerio Perrone, Cedric Archambeau, and Matthias Seeger. Cost-aware bayesian  
585 optimization. In *ICML Workshop on Automated Machine Learning*, 2020.

587 Mikhail Lifshits. Lectures on gaussian processes. In *Lectures on Gaussian Processes*, pp. 1–117.  
588 Springer, 2012.

589 Marco Locatelli. Bayesian algorithms for one-dimensional global optimization. *Journal of Global*  
590 *Optimization*, 10:57–76, 1997.

592 Romy Lorenz, Ricardo P Monti, Ines R Violante, Aldo A Faisal, Christoforos Anagnostopoulos,  
593 Robert Leech, and Giovanni Montana. Stopping criteria for boosting automatic experimental  
design using real-time fmri with bayesian optimization. *arXiv preprint arXiv:1511.07827*, 2015.

594 Anastasia Makarova, Huibin Shen, Valerio Perrone, Aaron Klein, Jean Baptiste Faddoul, Andreas  
595 Krause, Matthias Seeger, and Cedric Archambeau. Automatic termination for hyperparameter  
596 optimization. In *International Conference on Automated Machine Learning*, pp. 7–1. PMLR, 2022.  
597

598 Ruben Martinez-Cantin. Bayesian optimization with adaptive kernels for robot control. In *International  
599 Conference on Robotics and Automation*, 2017.

600 Vu Nguyen, Sunil Gupta, Santu Rana, Cheng Li, and Svetha Venkatesh. Regret for expected  
601 improvement over the best-observed value and stopping condition. In *Asian conference on machine  
602 learning*, pp. 279–294. PMLR, 2017.

603 Carl Edward Rasmussen and Christopher KI Williams. *Gaussian Processes for Machine Learning*.  
604 Cambridge University Press, 2006.

605 Jasper Snoek, Hugo Larochelle, and Ryan P Adams. Practical bayesian optimization of machine  
606 learning algorithms. *Advances in Neural Information Processing Systems*, 2012.

607 Niranjan Srinivas, Andreas Krause, Sham M Kakade, and Matthias Seeger. Gaussian process opti-  
608 mization in the bandit setting: No regret and experimental design. *arXiv preprint arXiv:0912.3995*,  
609 2009.

610 Joaquin Vanschoren, Jan N Van Rijn, Bernd Bischl, and Luis Torgo. Openml: networked science in  
611 machine learning. *ACM SIGKDD Explorations Newsletter*, 15(2):49–60, 2014.

612 Martin L Weitzman. Optimal search for the best alternative. *Econometrica*, 1979.

613 James Wilson. Stopping bayesian optimization with probabilistic regret bounds. *Advances in Neural  
614 Information Processing Systems*, 37:98264–98296, 2024.

615 Qian Xie, Raul Astudillo, Peter Frazier, Ziv Scully, and Alexander Terenin. Cost-aware bayesian  
616 optimization via the pandora’s box gittins index. *Advances in Neural Information Processing  
617 Systems*, 37:115523–115562, 2024.

618 Yichi Zhang, Daniel W Apley, and Wei Chen. Bayesian optimization for materials design with mixed  
619 quantitative and qualitative variables. *Scientific Reports*, 2020.

620 Lucas Zimmer, Marius Lindauer, and Frank Hutter. Auto-pytorch tabular: Multi-fidelity metalearning  
621 for efficient and robust autodl. *IEEE Transactions on Pattern Analysis and Machine Intelligence*,  
622 43(9):3079 – 3090, 2021.

623

624

625

626

627

628

629

630

631

632

633

634

635

636

637

638

639

640

641

642

643

644

645

646

647

648 A LLM USAGE DISCLOSURE  
649650 We used large language models (LLMs) to assist with writing and editing this paper (e.g., im-  
651 proving clarity and readability of drafts). LLMs were also used to help polish proofs, to facilitate  
652 experiment scripting, and to generate plotting code. All technical content, research ideas, and final  
653 implementations were developed, verified, and approved by the authors.  
654655 B THEORETICAL ANALYSIS AND CALCULATIONS  
656657 In the following lemma, we prove a point-wise lower bound on the expected improvement before  
658 stopping for our recommended pairing of PBGI/LogEIPC stopping rule paired with either PBGI or  
659 LogEIPC acquisition function.<sup>5</sup>  
660661 **Lemma 1.** *Let  $X$  be compact, and let  $f : X \rightarrow \mathbb{R}$  be a random function with prior mean  $\mu(\cdot)$ .  
662 Consider a Bayesian optimization algorithm that begins at some initial point  $x_1 \in X$  with cost  
663  $C = c(x_1)$ , acquires subsequent points using either the PBGI or LogEIPC acquisition function, and  
664 terminates according to the PBGI/LogEIPC stopping rule. Let  $\tau = \min_{t \geq 1} \{\sup_{x \in X} \alpha_t^{\text{LogEIPC}}(x) <  
665 0\}$  be the algorithm's stopping time, and denote the posterior expected improvement function by  
666  $\alpha_t^{\text{EI}}(x) = \text{EI}_{f|x_{1:t}, y_{1:t}}(x; y_{1:t}^*)$ . Then, for all  $t < \tau$ ,  $\alpha_t^{\text{EI}}(x_{t+1}) \geq c(x_{t+1})$ .*  
667668 *Proof.* While stopping has not occurred, meaning  $t < \tau$ , by the stopping criteria definition we have  
669  $\max_{x \in X} \alpha_t^{\text{EI}}(x)/c(x) \geq 1$ . Hence, there exists at least one point with  $\alpha_t^{\text{EI}}(x)/c(x) \geq 1$ . We now  
670 argue for each algorithm.671 *PBGI.* For each  $x$  we defined a threshold  $\alpha_t^{\text{PBGI}}(x)$  by  $\text{EI}_{f|x_{1:t}, y_{1:t}}(x; \alpha_t^{\text{PBGI}}(x)) = c(x)$ . Since  
672  $\text{EI}_{f|x_{1:t}, y_{1:t}}$  is increasing in its second argument,  
673

674 
$$y_{1:t}^* \geq \alpha_t^{\text{PBGI}}(x) \iff \alpha_t^{\text{EI}}(x)/c(x) \geq 1. \quad (12)$$

675 The existence of a point with ratio at least 1 therefore implies that the set  $\mathcal{S}_t = \{x : y_{1:t}^* \geq \alpha_t^{\text{PBGI}}(x)\}$   
676 is non-empty. PBGI chooses  $x_{t+1}$  with the *smallest* threshold, and thus  
677

678 
$$\alpha_t^{\text{EI}}(x_{t+1}) = \text{EI}_{f|x_{1:t}, y_{1:t}}(x_{t+1}; y_{1:t}^*) \geq \text{EI}_{f|x_{1:t}, y_{1:t}}(x_{t+1}; \alpha_t^{\text{PBGI}}(x_{t+1})) = c(x_{t+1}). \quad (13)$$

680 *(Log)EIPC.* By definition  $x_{t+1}$  maximizes  $\log(\alpha_t^{\text{EI}}(x)/c(x))$  and  $\alpha_t^{\text{EI}}(x)/c(x)$ , hence  $\alpha_t^{\text{EI}}(x_{t+1}) \geq  
681 c(x_{t+1})$ .  
682683 Thus for both algorithms, we have  
684

685 
$$\alpha_t^{\text{EI}}(x_{t+1}) \geq c(x_{t+1}), \quad \text{for all } t < \tau. \quad (14)$$

686  $\square$   
687688 We can now use Lemma 1 to prove the following theorem, where we show that our PBGI/LogEIPC  
689 stopping rule (paired with the PBGI or LogEIPC acquisition function) also achieves cost-adjusted  
690 simple regret no worse than a naive baseline—stopping-immediately (*Immediate*). Notably, this  
691 guarantee may not hold for other acquisition–stopping rule pairings. Moreover, in the worst case, this  
692 is the best guarantee we can hope for—for instance, the evaluation costs can be uniformly high and  
693 no point is worth evaluating.  
694695 **Theorem 2.** *Consider the setting and algorithm specified in Lemma 1. Let  $U := \mu(x_1) -$   
696  $\mathbb{E}[\min_{x \in X} f(x)] < \infty$ , then the algorithm's expected cost-adjusted simple regret is bounded by*  
697

698 
$$\mathbb{E} \left[ y_{1:\tau}^* - \min_{x \in X} f(x) + \sum_{t=1}^{\tau} c(x_t) \right] \leq \mathbb{E} \left[ \underbrace{y_1 - \min_{x \in X} f(x) + c(x_1)}_{\text{cost-adjusted regret of immediate stopping}} \right] = U + C. \quad (11)$$
  
699  
700

701 <sup>5</sup>In fact, any acquisition function (e.g., expected improvement-cost (EIC) (Hu et al., 2025)) that ensures the  
one-step expected improvement is worth the evaluation cost before the stopping time  $\tau$  can apply here.

702 *Proof.* We treat the two algorithms—meaning, the two acquisition function and stopping rule pairs—  
703 together and write  $\mathcal{F}_t = \sigma(\{x_i, y_i\}_{i=1}^t)$  for the filtration generated by the observations. Since we  
704 are minimizing, the one-step improvement after iteration  $t$  is  $y_{1:t-1}^* - y_{1:t}^*$ , where recall that  $y_{1:t}^* =$   
705  $\min_{1 \leq i \leq t} y_i$ . By our assumption about the random function  $f$ ,  $\mathbb{E}[y_{1:1}^*] = \mu(x_1)$  and the quantity  
706  $y_{1:1}^* - \min_{x \in X} f(x)$  has finite expectation  $U < \infty$ . Denote the posterior expected improvement  
707 function as  $\alpha_t^{\text{EI}}(x) = \text{EI}_{f|x_{1:t}, y_{1:t}}(x; y_{1:t}^*)$ .

708 By Lemma 1,  $c(x_t) \leq \alpha_{t-1}^{\text{EI}}(x_t)$  for all  $t \leq \tau$ . Set  $\Delta_t = y_{1:t-1}^* - y_{1:t}^* \geq 0$  for  $2 \leq t \leq \tau$ . Conditional  
709 on  $\mathcal{F}_{t-1}$  and the choice of  $x_t$ , we have  
710

$$711 \mathbb{E}[\Delta_t \mid \mathcal{F}_{t-1}, x_t] = \alpha_{t-1}^{\text{EI}}(x_t). \quad (15)$$

712 Taking expectations and summing up from 2 to  $\tau$ ,

$$\begin{aligned} 714 \mathbb{E}\left[\sum_{t=2}^{\tau} \alpha_{t-1}^{\text{EI}}(x_t)\right] &= \mathbb{E}\left[\sum_{t=2}^{\infty} \mathbf{1}_{\{t \leq \tau\}} \alpha_{t-1}^{\text{EI}}(x_t)\right] \\ 715 &= \mathbb{E}\left[\sum_{t=2}^{\infty} \mathbf{1}_{\{t \leq \tau\}} \mathbb{E}[\Delta_t \mid \mathcal{F}_{t-1}, x_t]\right] \\ 716 &= \mathbb{E}\left[\sum_{t=2}^{\infty} \mathbf{1}_{\{t \leq \tau\}} \Delta_t\right] \quad (\text{tower property}) \\ 717 &= \mathbb{E}\left[\sum_{t=2}^{\tau} \Delta_t\right] = \mathbb{E}[y_{1:1}^* - y_{1:\tau}^*]. \end{aligned} \quad (16)$$

725 Summing (14) over  $t \leq \tau$ , taking expectations, and applying (16), we have  
726

$$727 \mathbb{E}\left[\sum_{t=2}^{\tau} c(x_t)\right] \leq \mathbb{E}\left[\sum_{t=2}^{\tau} \alpha_{t-1}^{\text{EI}}(x_t)\right] \leq \mathbb{E}[y_{1:1}^* - y_{1:\tau}^*]. \quad (17)$$

730 Adding the term  $y_{1:\tau}^*$  on both sides of (17) gives

$$731 \mathbb{E}\left[y_{1:\tau}^* + \sum_{t=2}^{\tau} c(x_t)\right] \leq \mathbb{E}[y_{1:1}^*].$$

734 Finally, adding  $c(x_1)$  to both sides and subtracting  $\mathbb{E}[\min_{x \in X} f(x)]$  yields  
735

$$\begin{aligned} 736 \mathbb{E}\left[y_{1:\tau}^* - \min_{x \in X} f(x) + \sum_{t=1}^{\tau} c(x_t)\right] &\leq \mathbb{E}\left[y_{1:1}^* - \min_{x \in X} f(x) + c(x_1)\right] \\ 737 &= \mathbb{E}\left[y_1 - \min_{x \in X} f(x) + c(x_1)\right] \\ 738 &= \mu(x_1) - \mathbb{E}\left[\min_{x \in X} f(x)\right] + \mathbb{E}[c(x_1)] \\ 739 &= U + C, \end{aligned}$$

745 since  $\mathbb{E}[y_1] = \mu(x_1)$ ,  $C = c(x_1)$ , and  $U = \mu(x_1) - \mathbb{E}[\min_{x \in X} f(x)]$ . This is exactly (11).  $\square$

746 **Remark 5.** The quantities  $U$  and  $C$  depend on the choice of the initial point  $x_1$ . Choosing  $x_1$  to  
747 minimize  $\mu(x_1) + c(x_1)$  yields a tighter bound.  
748

749 **Remark 6.** In practice, one may center the objective by replacing  $f(x)$  with  $f(x) - \mu(x)$  and then  
750 using a zero-mean GP prior. This changes only the parameterization of the posterior mean (which  
751 can be shifted back by  $\mu(x)$ ) and does not affect the implementation of the acquisition functions or  
752 stopping rules.

753 **Corollary 3.** Consider the setting and algorithm specified in Lemma 1. Then the expected cumulative  
754 cost of the algorithm is bounded by  $\mathbb{E}[\sum_{t=1}^{\tau} c(x_t)] \leq U + C$ . Further, if evaluation costs are  
755 uniformly bounded below by a constant  $c_0 > 0$ , i.e.,  $c(x) \geq c_0, \forall x \in X$ , then for any  $\delta \in (0, 1)$ , the  
756 algorithm terminates in at most  $\frac{U+C}{\delta \cdot c_0}$  iterations with probability  $1 - \delta$ .

756 *Proof.* Immediately by Theorem 2 and the fact that  $y_{1:\tau}^* - \min_{x \in X} f(x) > 0$  pointwise, we have  
 757 that the expected cumulative cost of the algorithm  
 758

$$759 \mathbb{E} \left[ \sum_{t=1}^{\tau} c(x_t) \right] \leq U + C. \quad (18)$$

760 By Markov's inequality, for any  $\delta \in (0, 1)$ ,

$$763 \Pr \left[ \sum_{t=1}^{\tau} c(x_t) \leq \frac{U + C}{\delta} \right] \geq 1 - \delta.$$

764 Since  $c(x_t) \geq c_0$  for all  $t < \tau$ , it follows that

$$765 \tau = \sum_{t=1}^{\tau} 1 \leq \sum_{t=1}^{\tau} \frac{c(x_t)}{c_0} = \frac{1}{c_0} \sum_{t=1}^{\tau} c(x_t).$$

766 Therefore,

$$767 \Pr \left[ \tau \leq \frac{U + C}{\delta \cdot c_0} \right] \geq \Pr \left[ \frac{1}{c_0} \sum_{t=1}^{\tau} c(x_t) \leq \frac{U + C}{\delta \cdot c_0} \right] = \Pr \left[ \sum_{t=1}^{\tau} c(x_t) \leq \frac{U + C}{\delta} \right] \geq 1 - \delta.$$

□

768 **Corollary 4.** Consider the setting, algorithm, and notation specified in Lemma 1 and Theorem 2, but  
 769 with costs rescaled by a factor  $\lambda > 0$ : both the acquisition values and the stopping conditions are  
 770 computed using  $\lambda c(\cdot)$ . If the cost-scaling factor is set to  $\lambda = \frac{U}{B-C}$ , then the algorithm's expected  
 771 cumulative unscaled cost satisfies  $\mathbb{E}[\sum_{t=1}^{\tau} c(x_t)] \leq B$ .

772 *Proof.* Since the Bayesian optimization algorithm considers the post-scaling cost, by Theorem 2 and  
 773 the fact that  $y_{1:\tau}^* - \min_{x \in X} f(x) > 0$  pointwise, we have

$$774 \mathbb{E} \left[ \sum_{t=1}^{\tau} \lambda \cdot c(x_t) \right] \leq \mathbb{E} \left[ y_{1:\tau}^* - \min_{x \in X} f(x) + \sum_{t=1}^{\tau} \lambda \cdot c(x_t) \right] \leq \mu(x_1) - \mathbb{E} \left[ \min_{x \in X} f(x) \right] + \lambda C = U + \lambda C. \quad (19)$$

775 Since  $\lambda = U/(B - C)$ , we have

$$776 \mathbb{E} \left[ \sum_{t=1}^{\tau} c(x_t) \right] \leq \frac{U + \lambda C}{\lambda} = \frac{U}{\lambda} + C = B.$$

□

777 **Remark 7.** In this paper, we focus on the setting where  $f$  is drawn from a Gaussian process, i.e.,  
 778  $f \sim \mathcal{GP}(\mu(\cdot), K)$ . In this case, the term  $U = \mu(x_1) - \mathbb{E}[\min_{x \in X} f(x)]$  can be further bounded  
 779 above using classical results on the expected supremum/infimum of Gaussian processes; see, for  
 780 example, Lifshits (2012, Theorem 10.1).

## 781 C EXPERIMENTAL SETUP

801 All experiments are implemented based on BoTorch (Balandat et al., 2020). Each Bayesian optimization  
 802 procedure is initialized with  $2(d + 1)$  random samples, where  $d$  is the dimension of  
 803 the search domain. For Bayesian regret experiments, we follow the standard practice to generate  
 804 the initial random samples using a quasirandom Sobol sequence. For empirical experiments, we  
 805 randomly sample configuration IDs from a fixed pool of candidates—2,000 for LC-Bench and 32,768  
 806 for NATS-Bench. All computations are performed on CPU.

807 Each experiment is repeated with 50 random seeds, and we report the mean with error bars, given by  
 808 two times the standard error, for each stopping rule. We also impose a cap on the number of iterations:  
 809 100 for 1D Bayesian regret, 500 for 8D Bayesian regret, and 200 for empirical experiments. If a  
 810 stopping rule is not triggered before reaching this cap, we treat the stopping time as equal to the cap.

810    **Gaussian process models.** For all experiments, we follow the standard practice to apply Matérn  
 811    kernels with smoothness 5/2 and length scales learned from data via maximum marginal likelihood  
 812    optimization, and standardize input variables to be in  $[0, 1]^d$ . For empirical experiments, we stan-  
 813    dardize output variables to be zero-mean and unit-variance, but not for Bayesian regret experiments.  
 814    In this work, we consider the noiseless setting and set the fixed noise level to be  $10^{-6}$ . In the  
 815    unknown-cost experiments, we follow Astudillo et al. (2021) to model the objective and the logarithm  
 816    of the cost function using independent Gaussian processes.

817    **Acquisition function optimization.** For the 1D Bayesian regret experiments, we optimize over  
 818    10,001 grid points. For the 8D Bayesian regret experiment, we use BoTorch’s ‘gen\_candidates\_torch’,  
 819    a gradient-based optimizer for continuous acquisition function maximization, as it avoids reproducibil-  
 820    ity issues caused by internal randomness in the default scipy optimizer. For the empirical experiments,  
 821    since LCBench and NATS-Bench provide only 2,000 and 32,768 configurations respectively, we  
 822    optimize the acquisition function by simply applying an argmin/argmax over the acquisition values  
 823    of the unevaluated configurations, without using any gradient-based methods.

824    **Acquisition function and stopping rule parameters.** For PBGI, we follow Xie et al. (2024) to  
 825    compute the Gittins indices using 100 iterations of bisection search without any early stopping or  
 826    other performance and reliability optimizations.

827    For UCB/LCB-based acquisition functions and stopping rules, we follow the original GP-UCB paper  
 828    Srinivas et al. (2009) and the choice in UCB/LCB based stopping rules (Makarova et al., 2022;  
 829    Ishibashi et al., 2023) to use the schedule  $\beta_t = 2 \log(dt^2\pi^2/6\delta)$ , where  $d$  is the dimension. We also  
 830    adopt their choice of  $\delta = 10^{-1}$  and a scale-down factor of 5.

831    For SRGap-med, which stops when the simple regret gap falls below  $\chi$  times the median of its initial  
 832     $T = 20$  values, we set  $\chi = 0.1$  in the empirical experiments, instead of the default value  $\chi = 0.01$   
 833    recommended in the literature. This adjustment was made because SRGap-med tends to stop too late  
 834    on the LCBench datasets, likely due to the relatively small initial regret values and insignificant drop  
 835    over time.

836    For PRB, we follow Wilson (2024) to use the schedule  $N_t = \max(\lceil 64 * 1.5^{t-1} \rceil, 1000)$  for number  
 837    of posterior samples, risk tolerance  $\delta = 0.05$ . The error bound  $\epsilon$  is set to be 0.1 for Bayesian regret  
 838    experiments and 0.5% of the best test error (here, the misclassification rate) among all configurations  
 839    for the empirical experiments.

840    For the 8D Bayesian regret experiments, for all acquisition-value-based stopping rules, we apply  
 841    moving average over 20 iterations to mitigate the fluctuations due to the imperfect acquisition function  
 842    optimization. Figure 4 illustrates the challenges these oscillations pose when computing stopping  
 843    rule statistics and shows the improvement with moving average. For consistency, we also apply the  
 844    20-iteration averaging to the non-acquisition-value-based GSS and Convergence baselines.

845    **Omitted baselines.** We omit the KG acquisition function and stopping rule due to its high compu-  
 846    tational cost, as they are shown to be computationally intensive in the runtime experiments of Xie  
 847    et al. (2024).

848    **Objective functions: Bayesian regret.** In all Bayesian regret experiments, each objective function  
 849     $f$  is sampled from a Gaussian process prior with a Matérn 5/2 kernel and a length scale of 0.1, using  
 850    a different seed in each of the 50 trials.

851    **Objective functions: empirical.** In the empirical experiments, the validation error (scaled out  
 852    of 100) is used as the objective function during the Bayesian optimization procedure, while the  
 853    cost-adjusted simple regret is reported based on the corresponding test error.

854    **Cost functions: Bayesian regret.** In Bayesian regret experiments, we consider three types of  
 855    evaluation costs: uniform, linear, and periodic. These costs are normalized such that  $\mathbb{E}_{x \in [0, 1]^d} [c(x)]$   
 856    is approximately 1 and their expressions (prior to cost scaling) are given below.

857    In the *uniform* cost setting, each evaluation incurs a constant cost of 1.

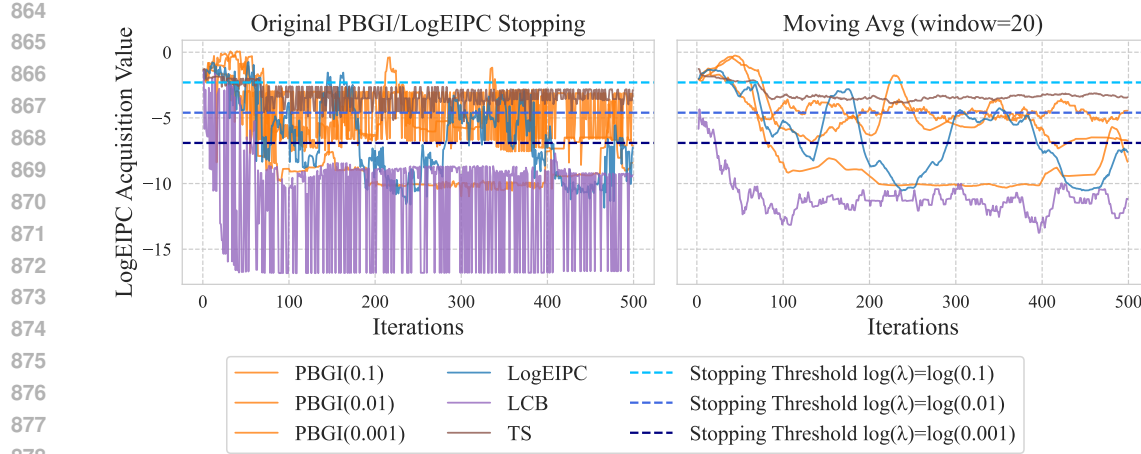


Figure 4: Comparison of the raw and moving-averaged PBGI/LogEIPC stopping rule signals (i.e., the LogEIPC acquisition values) in Bayesian regret 8D experiments for multiple acquisition functions, with linear cost and stopping thresholds at  $\log(0.1)$ ,  $\log(0.01)$  and  $\log(0.001)$ . *Left:* The unaveraged signals exhibits large, high-frequency fluctuations due to the difficulty of acquisition optimization in high dimensions. *Right:* Applying moving average (window=20) smooths these wiggles, yielding more stable stopping signals.

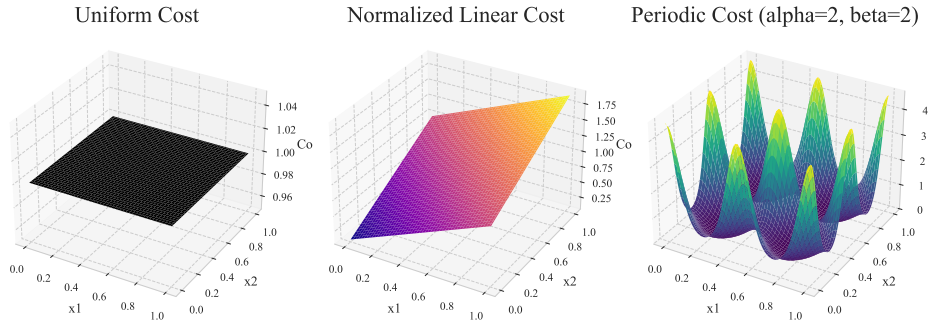


Figure 5: Surface plots of cost functions over  $[0, 1]^2$ : (Left) Uniform cost of 1 across domain. (Middle) Normalized linear cost increasing with the mean of  $x_1$  and  $x_2$ . (Right) Periodic cost with  $\alpha = 2$ ,  $\beta = 2$ , normalized by Bessel-based factor.

In the *linear* cost setting, the cost increases proportionally with the average coordinate value of the input:

$$\text{linear\_cost}(x) = \frac{1 + 20 \cdot \left( \frac{1}{d} \sum_{i=1}^d x_i \right)}{11}.$$

In the *periodic* cost setting, the evaluation cost fluctuates across the domain. Following Astudillo et al. (2021), we define the periodic cost as

$$\text{periodic\_cost}(x) = \frac{\exp \left( \frac{\alpha}{d} \sum_{i=1}^d \cos(2\pi\beta(x_i - x_i^*)) \right)}{\left[ I_0 \left( \frac{\alpha}{d} \right) \right]^d},$$

where  $x_i^*$  denotes the coordinate of the global optimum of  $f$ , and  $I_0$  is the modified Bessel function of the first kind, which acts as a normalization constant. We set  $\alpha = 2$  and  $\beta = 2$  to induce noticeable variation in cost across the domain, while ensuring that costly evaluations can still be worthwhile.

A visualization of the three cost functions is provided in Figure 5.

**Cost functions: empirical.** In the *unknown-cost* experiments, we treat runtime—meaning, the provided full model training time (200 epochs for LCbench and 90 epochs for NATS)—as evaluation costs (prior to cost scaling).

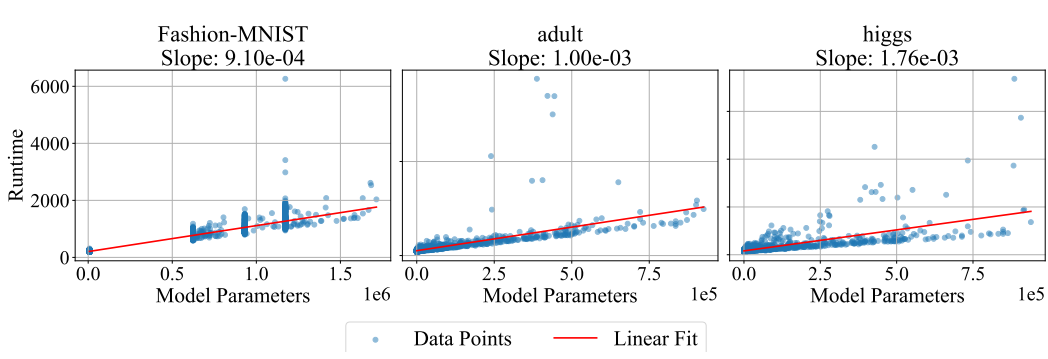


Figure 6: Empirical relationship between the number of model parameters and runtime for three LCBench datasets. Each subplot shows a scatter plot of actual runtime ( $y$ -axis) against number of model parameters ( $x$ -axis), along with a fitted linear regression line. The observed linear trend supports using 0.001 times the number of model parameters as a proxy for runtime. For *Fashion-MNIST* and *adult*, the fitted slopes are close to 0.001. The slope for *higgs* is slightly higher, possibly due to a few outliers.

In the *known-cost* experiments, for LCBench, we estimate the runtime cost from the number of model parameters  $p$ . Specifically, for the first three datasets in the six-dataset lite version, we use 0.001 times the number of model parameters as a proxy for runtime. This proxy is motivated by our observation of an approximately linear relationship between the number of model parameters and the actual runtime, with slope close to 0.001 (see Figure 6). For the full 35-dataset version, where the slope varies across datasets, we instead use a regression-derived coefficient  $\alpha$  and the proxy cost is  $\alpha p$ . Importantly, the number of model parameters can be computed in advance, before the Bayesian optimization procedure, based on the network structure and classification task, as we explain in detail below.

In a feedforward neural network like shapedmlpnet with shape ‘funnel’, the model parameters are determined by input size (number of features), output size (e.g., number of classes), number of layers, size of each layer. The input size and output size are given by:

- **Fashion-MNIST:**
  - Input dimension: 784 (each image has 28×28 pixels, flattened into a vector of length 784)
  - Number of Output Features (output\_feat): 10 (corresponding to 10 clothing categories)
- **Adult:**
  - Input Dimension: 14 (the dataset comprises 14 features, including both numerical and categorical attributes)
  - Number of Output Features: 1 (binary classification: income > 50K or  $\leq$  50K)
- **Higgs:**
  - Input Dimension: 28 (each instance has 28 numerical features)
  - Number of Output Features: 1 (binary classification: signal or background process)

The number of layers (num\_layers) and size of each layer (max\_unit) can be obtained from the configuration. With these information, we can compute the total number of model parameters (weights and biases) based on the layer-wise structure as follows:

$$\text{layer\_params}_{i \rightarrow i+1} = \text{layer}_i \cdot \text{layer}_{i+1} + \text{layer}_{i+1} \quad (\text{weights + biases}) \quad (20)$$

$$\text{model\_params} = \sum_{i=0}^{L-1} \text{layer\_params}_{i \rightarrow i+1} \quad (21)$$

$$\text{where } \text{layer}_0 = \text{input\_dim}, \quad \text{layer}_L = \text{output\_feat} \quad (22)$$

Similarly for NATS-Bench, we use  $\alpha \times F + \beta$  as a proxy for runtime (see Figure 7 for a visualization of the linear relationship), where  $F$  is the number of floating point operations (FLOPs). Specifically, for

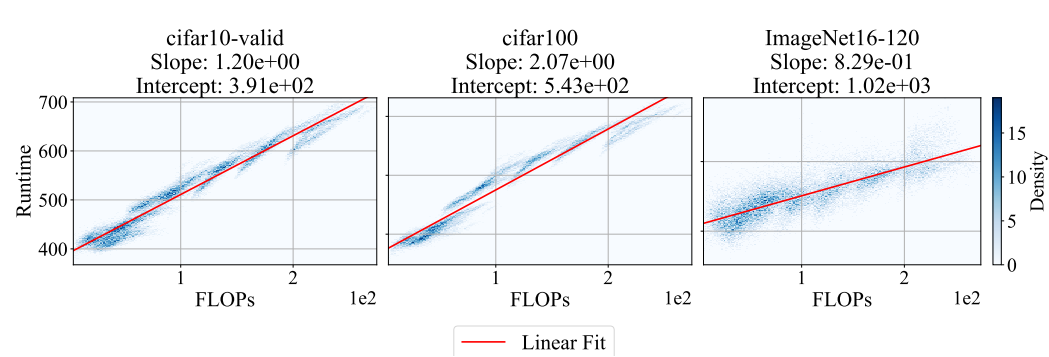


Figure 7: Empirical relationship between the number of FLOPs and runtime for the three NATS-Bench datasets. Each subplot shows a heatmap of actual runtime ( $y$ -axis) against number of FLOPs ( $x$ -axis), along with a fitted linear regression line. The observed linear trend supports using  $\alpha \times \#FLOPs + \beta$  as a proxy for runtime.

*cifar10-valid*, we set  $\alpha = 1, \beta = 400$ ; for *cifar100*, we set  $\alpha = 2, \beta = 550$ ; and for *ImageNet16-120*, we set  $\alpha = 1, \beta = 1000$ .

FLOPs can also be computed in advance, as it is determined solely by the architecture’s structure and the fixed input shape. Specifically, they are precomputed and stored for each architecture. Since each architecture corresponds to a deterministic computational graph and all inputs (e.g., CIFAR-10 images) have a fixed shape, the FLOPs required for a forward pass can be calculated analytically—without executing the model on data.

## D ADDITIONAL EXPERIMENT RESULTS

In this section, we present additional experimental results to further evaluate the performance of different acquisition-function–stopping-rule pairs across various settings. We also include alternative visualizations to aid interpretation of the results.

### D.1 RUNTIME COMPARISON

First, we compare the runtime between our PBGI/LogEIPC stopping rule with several baselines. We measure the CPU time (in seconds) of the computation of the stopping rule, excluding the acquisition function computation and optimization.

From results in Figure 8 we can see that our PBGI/LogEIPC stopping rule is roughly as efficient as SRGap-med and UCB–LCB. In contrast, PRB is significantly more time-consuming, as it involves optimizing over up to 1000 samples.

### D.2 ORDER OF STOPPING AND POSTERIOR UPDATES

Following the discussions in Section 3, we always compute our proposed stopping rule with respect to the optimal acquisition function value of the *next round*—namely, the one which is obtained after posterior updates have been performed. One could alternatively consider checking the stopping criteria *before* posterior updates, which is backward-looking rather than forward-looking. Figure 9 provides an empirical comparison between the two choices, showing that stopping *after* the posterior update leads to stronger empirical performance.

This suggests that the theoretical guarantee for the Gittins index policy in the correlated Pandora’s Box setting by Gergatsouli & Tzamos (2023), which is based on the *before-posterior-update* stopping, could potentially be improved by adopting the *after-posterior-update* stopping.

### D.3 ADDITIONAL EXPERIMENT RESULTS: EMPIRICAL

This subsection presents additional results for hyperparameter optimization on the LCbench datasets and neural architecture–size search on the three NATS-Bench datasets. For LCbench, we provide

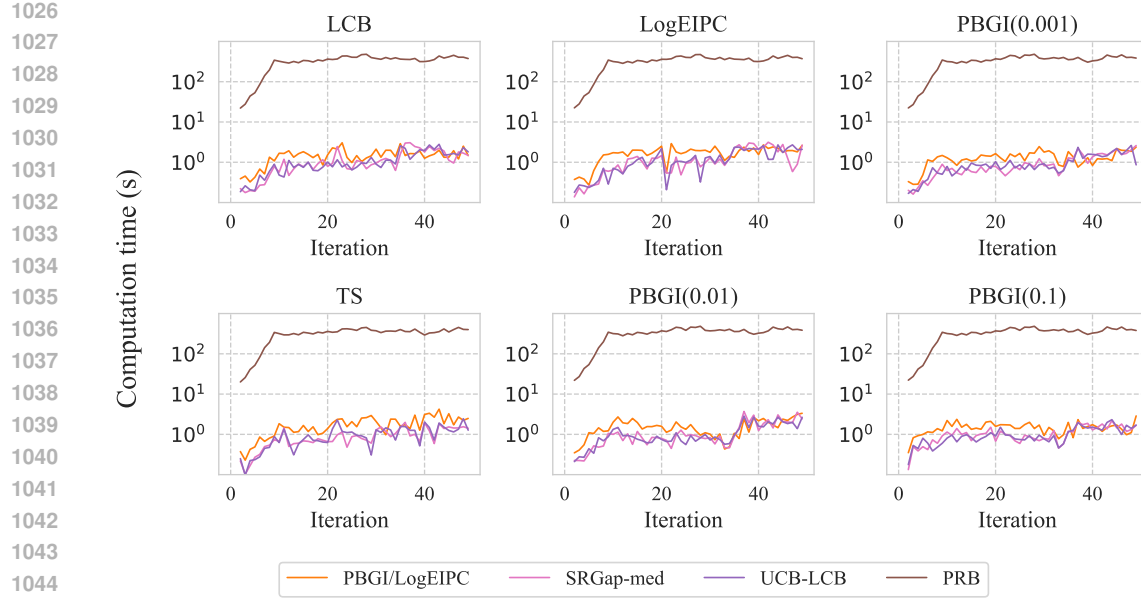


Figure 8: Evolution of per-iteration computation time (in log scale) for different stopping rules when paired with six acquisition policies on the 8-dimensional Bayesian regret benchmark. Each subplot shows the average runtime (in seconds) over 50 iterations under one acquisition function—LCB, Thompson Sampling, LogEIPC, PBGI( $\lambda = 10^{-1}$ ), PBGI( $\lambda = 10^{-2}$ ), and PBGI( $\lambda = 10^{-3}$ ). Curves correspond to four stopping criteria: our PBGI/LogEIPC stopping rule, SRGap-med, UCB-LCB, and the probabilistic regret bound (PRB). Convergence and GSS can be applied using only the best observed value and thus require no additional computation time, thus they are omitted here. LogEIPC-med relies on the same underlying statistical computations as the LogEIPC rule, and therefore its runtime is not measured separately. The results show that PRB incurs significant computational overhead compared to other stopping rules.

results for the first three datasets from the six-dataset lite version of the benchmark: Fashion-MNIST, adult, and higgs under alternative settings (fixed budget, actual runtime, and unknown cost), along with an alternative visualization. We also include per-dataset results under the proxy-runtime setting for the full set of 35 datasets.

**Simple regret under the fixed-budget setting.** To isolate the effect of the acquisition function on cost-adjusted regret, we report the simple regret of several acquisition functions in the fixed-budget setting. We compare LogEIPC, PBGI, LCB, and TS, and additionally include PBGI-D with our recommended choice  $\lambda_0 = U/(B - C)$  from Section 3.1.1, where  $U = 50$  (reflecting the [0,100] range of classification accuracy) and  $B - C = 10,000$  (corresponding to a budget after initial evaluation of 10,000 seconds, or roughly 3 hours). Cost-aware methods (LogEIPC and the PBGI variants) outperform cost-unaware ones (UCB and TS), with PBGI at smaller  $\lambda$  consistently better than LogEIPC. This mirrors the findings of Xie et al. (2024) and helps explain the strong performance of the matched PBGI combination in our main experiments.

**Number of trials where stopping fails.** We count the number of trials in which a stopping rule fails to trigger within our iteration cap of 200 and present the results in Table 1. From the table, we observe that on datasets from the NATS benchmark, regret-based and acquisition-based stopping rules—except for ours—often fail to stop early. On LCBench datasets, some regret-based stopping rules such as SRGap-med and UCB-LCB also frequently exceed the cap. In contrast, our stopping rule consistently stops early, which aligns with our theoretical result in Corollary 4.

**Alternative visualization: cost-adjusted regret vs iteration.** We provide an alternative visualization of cost-adjusted simple regret by plotting its mean and error bars at fixed iterations, along with the mean and error bars of the stopping iterations for each rule. This allows us to compare the

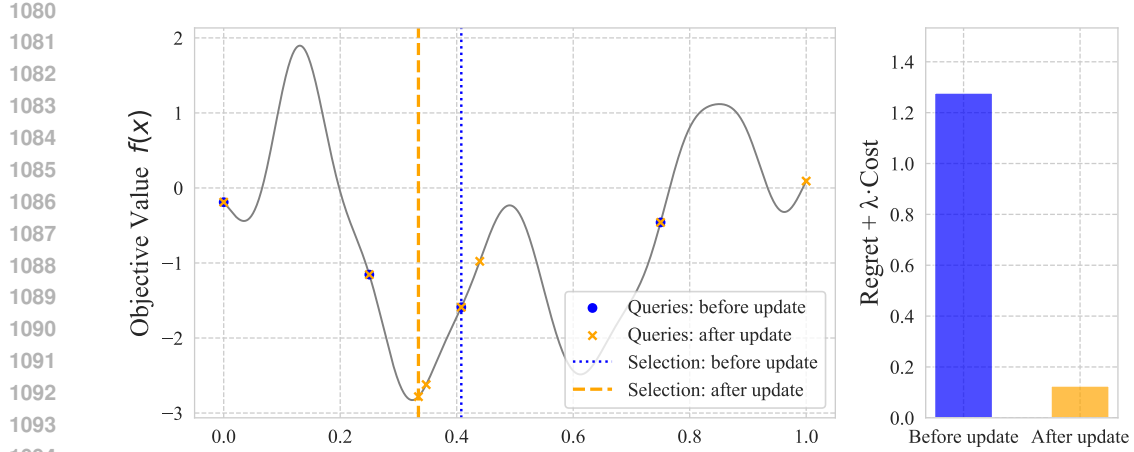


Figure 9: Illustration of a single draw from a Matérn-5/2 Gaussian process on  $[0, 1]$  with lengthscale 0.1, optimized using PBGI acquisition function under uniform cost and cost-scaling factor  $\lambda = 0.01$ . We compare two variants of PBGI stopping rules: the *before-posterior-update* (this-round) stopping rule and the *after-posterior-update* (next-round) stopping rule. **Left:** The latent objective function (solid gray) and evaluation sequences for *before-posterior-update* stopping (blue circles) and *after-posterior-update* stopping (orange crosses). The dotted blue line and the dashed orange line mark the best observed value under each respective rule. **Right:** Cost-adjusted regret for each stopping rule. In this example, *after-posterior-update* stopping achieves strictly lower cost-adjusted regret despite performing more evaluations.

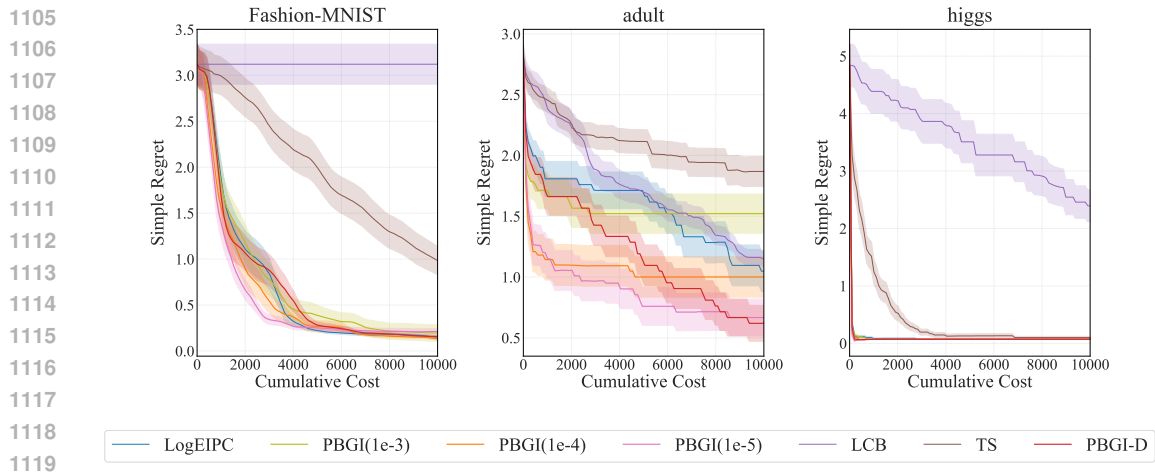


Figure 10: Comparison of simple regret of five acquisition functions: LogEIPC, PBGI( $\lambda = 10^{-4}$ ), LCB, TS, and PBGI-D on LCBench datasets, using scaled proxy runtime as evaluation cost. We can see that indeed the cost-aware LogEIPC and PBGI outperforms the cost-unaware UCB and TS. PBGI-D with out recommended  $\lambda_0$  is also competitive.

performance of adaptive stopping rules not only against the hindsight-optimal adaptive stopping but also against the hindsight-optimal fixed-iteration stopping.

As shown in the empirical setting in Figures 11 to 16, cost-adjusted regret generally decreases in the early iterations and then increases. The turning point is exactly the hindsight-optimal fixed-iteration stopping point, and our PBGI/LogEIPC stopping rule consistently performs close to this optimum, particularly when paired with the PBGI acquisition function.

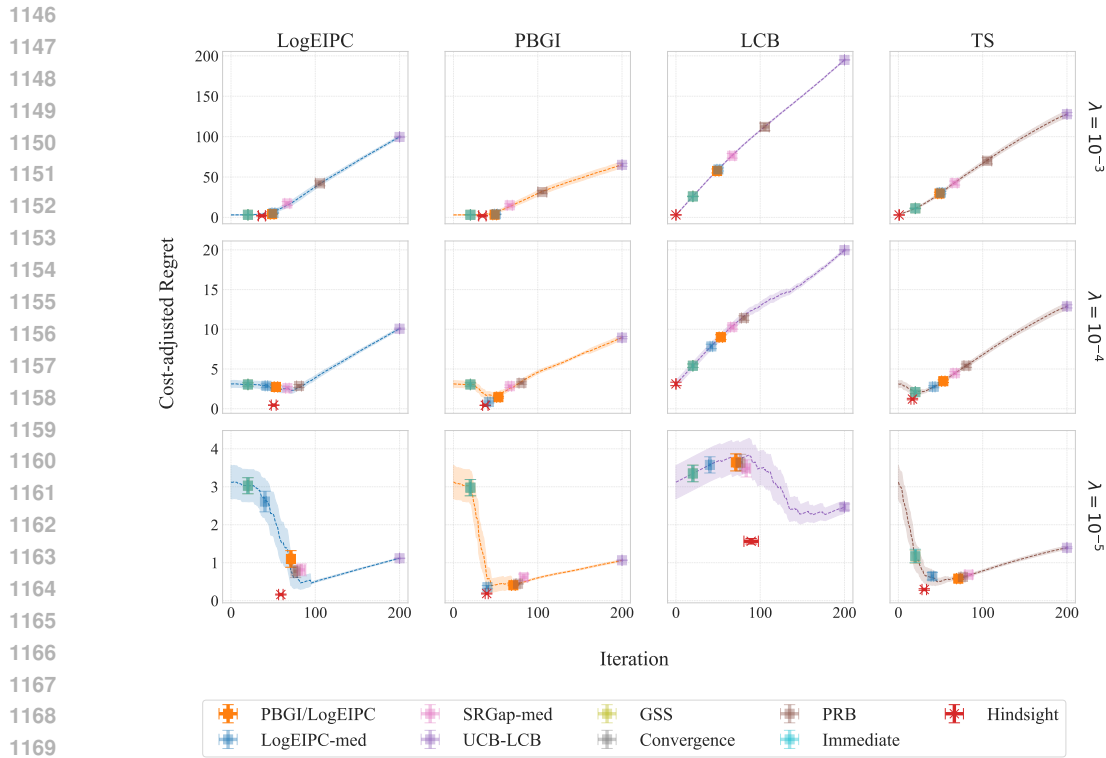
**Cost model mismatch: proxy runtime vs actual runtime.** In the known-cost setting of hyperparameter tuning, a practical approach is to use a proxy for runtime as the evaluation cost during the Bayesian optimization procedure. In our case, we use the number of model parameters scaled

1134 Table 1: Number of trials (out of 50) where each stopping rule failed to trigger within 200 iterations,  
 1135 for each dataset in the LCBench (first three) and NATS (last three) benchmarks and each acquisition  
 1136 function. Results are identical across acquisition functions.

1137

1138 <b>Dataset</b>	1139 <b>PBGI</b>	1140 <b>LogEIPC-med</b>	1141 <b>SRGap-med</b>	1142 <b>UCB-LCB</b>	1143 <b>GSS</b>	1144 <b>Convergence</b>	1145 <b>PRB</b>
Fashion-MNIST	0	0	0	50	0	0	0
adult	5	0	7	38	0	0	6
higgs	0	0	31	50	0	0	0
Cifar10	0	32	50	50	0	0	26
Cifar100	3	17	50	50	0	0	2
ImageNet	0	23	50	50	0	0	0

1146



1166

1167

1168 Figure 11: Comparison of cost-adjusted simple regret across acquisition function and stopping rule  
 1169 pairs on the *Fashion-MNIST* dataset. The objective function is the validation error, and the evaluation  
 1170 cost is the proxy runtime, scaled by three different cost-scaling factors  $\lambda = 10^{-3}, 10^{-4}, 10^{-5}$ . We  
 1171 can see that the PBGI/LogEIPC stopping rule consistently achieves cost-adjusted regret close to the  
 1172 hindsight optimal adaptive stopping as well as the hindsight optimal fixed-iteration stopping when  
 1173 paired with the PBGI acquisition function, though not always the best.

1174

1175

1176

1177 by a constant factor, which can be known in advance and has been shown to correlate well with  
 1178 the actual runtime. However, for reporting performance, one may prefer to use the actual runtime  
 1179 to better reflect real-world cost. To assess the impact of this cost model mismatch, we compare  
 1180 the cost-adjusted simple regret obtained when evaluation costs are computed using either the proxy  
 1181 runtime or the actual runtime. As shown in Figure 17, our PBGI/LogEIPC stopping rule remains  
 1182 close to the hindsight optimal even when there is a mismatch, although its ranking may shift slightly  
 1183 (e.g., from best to second-best on the *higgs* dataset).

1184

1185

1186

1187

**Unknown-cost.** Astudillo et al. (2021, Proposition 2) proposed modeling unknown cost  $c(x)$  via

$$\mathbb{E}[1/c(x)]^{-1} = \exp(\mu_{\ln c}(x) - (\sigma_{\ln c}(x))^2/2). \quad (23)$$

An alternative is

$$\mathbb{E}[c(x)] = \exp(\mu_{\ln c}(x) + (\sigma_{\ln c}(x))^2/2). \quad (24)$$

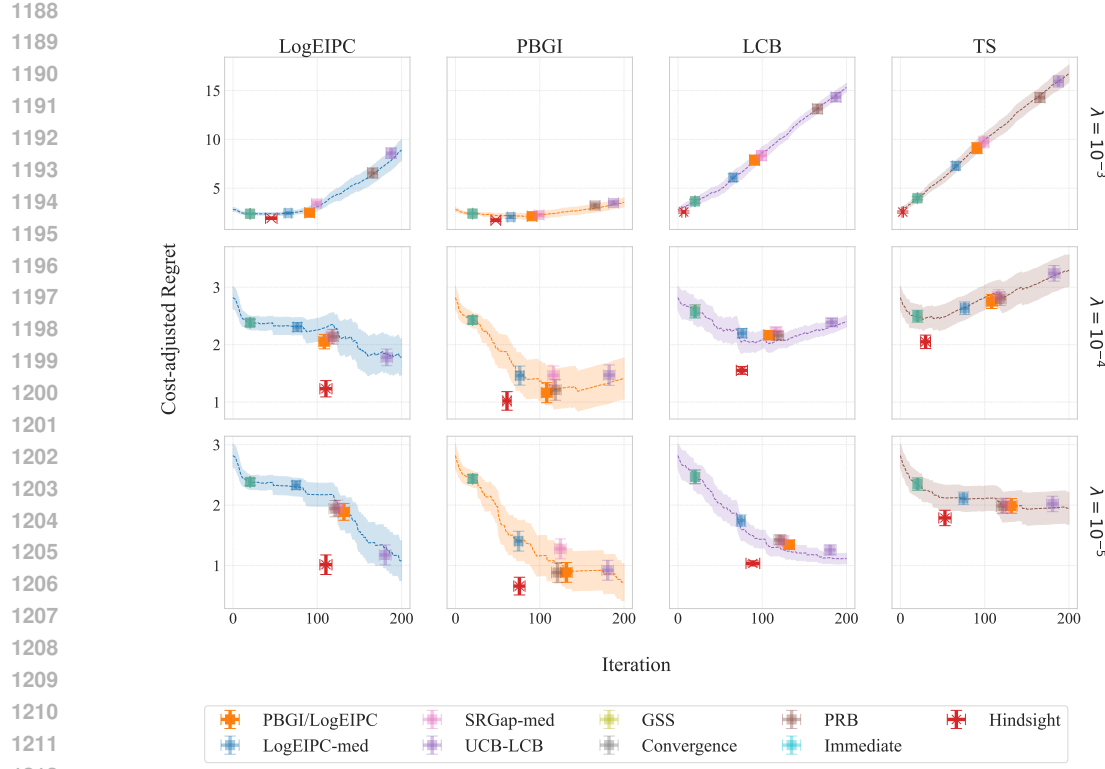


Figure 12: Comparison of cost-adjusted simple regret across acquisition function and stopping rule pairs on the *adult* dataset. The objective function is the validation error, and the evaluation cost is the proxy runtime, scaled by three different cost-scaling factors  $\lambda = 10^{-3}, 10^{-4}, 10^{-5}$ . We can see that the PBGI/LogEIPC stopping rule consistently achieves the cost-adjusted regret close to hindsight optimal adaptive stopping and hindsight optimal fixed-iteration stopping when paired with the PBGI or TS acquisition function, particularly with PBGI.

The difference in sign before the variance term reflects how each formulation handles predictive uncertainty: (23) encourages more exploration than (24). For PBGI under the unknown-cost setting, it is more natural to replace  $c(x)$  in (5) with  $\mathbb{E}[c(x)]$  using (24), as this aligns with how costs enter the root-finding problem. For LogEIPC, both variants are possible—we refer to the (23) version as *LogEIPC-inv* and the (24) version as *LogEIPC-exp*. However, equivalence between PBGI and LogEIPC stopping rules and our theoretical guarantees hold only with (24) but not with (23). Accordingly, we use (24) for both methods in our experiments to maintain consistency and preserve this equivalence. Figure 18 shows performance of acquisition function and stopping rule pairs under the unknown-cost setting, which are qualitatively similar to the known-cost setting.

**Cost-adjusted simple regret of all LCBench datasets.** Due to space constraints, for LCBench, Figure 3 in the main text reports min–max normalized cost-adjusted simple regret, defined as

$$\frac{r - r_{\min}}{r_{\max} - r_{\min}},$$

where  $r$  denotes cost-adjusted regret of a given acquisition function–stopping rule pair, and  $r_{\min}$  and  $r_{\max}$  are the minimum (including the hindsight optimal) and maximum cost-adjusted regret across all pairs. This normalization enables aggregation across datasets with different regret scales.

Here we present the *unnormalized* bar-plot results for each LCBench dataset (OpenML dataset size in parentheses) under all three cost-scaling parameters in Figures 19 to 21. As discussed in the main text, our PBGI/LogEIPC stopping rule—when paired with either PBGI or LogEIPC—achieves competitive performance on roughly 75% of the 35 datasets. However, it performs consistently poorly across all three  $\lambda$  values on the following tasks: *Amazon\_employee\_access* (32769), *Australian* (690), *KDDCup09\_appetency* (50000), *cnae-9* (1080), *credit-g* (1000), *fabert* (8237), and *vehicle* (846). Two additional datasets, *mfeat-factors* (2000) and *jasmine* (2984), show acceptable performance

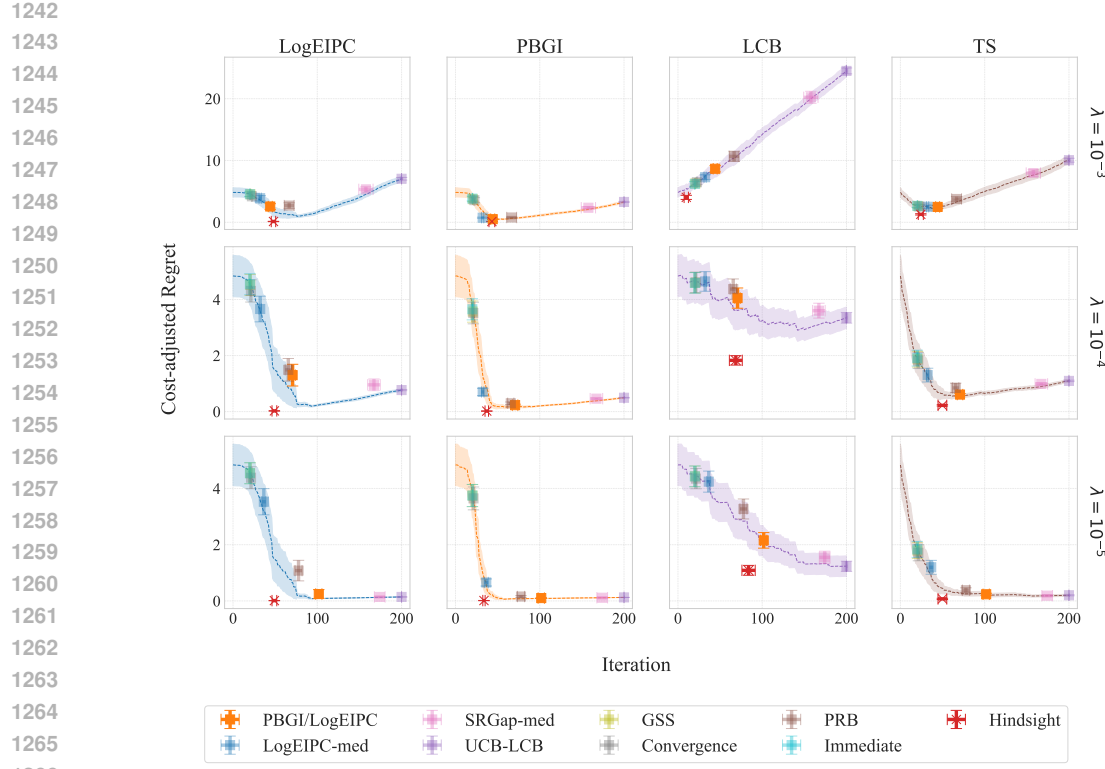


Figure 13: Comparison of cost-adjusted simple regret across acquisition function and stopping rule pairs on the *higgs* dataset. The objective function is the validation error, and the evaluation cost is the proxy runtime, scaled by three different cost-scaling factors  $\lambda = 10^{-3}, 10^{-4}, 10^{-5}$ . We can see that the PBGI/LogEIPC stopping rule consistently achieves the best cost-adjusted regret when paired with the LogEIPC, PBGI, or TS acquisition function, particularly with PBGI. These pairs not only approach the hindsight optimal adaptive stopping but also perform comparably to the hindsight optimal fixed-iteration stopping.

only when  $\lambda = 10^{-5}$ , and we conjecture that their relatively small dataset sizes (fewer than 10000 instances) may contribute to model misspecification and degraded performance at larger  $\lambda$ . The only exceptions to this size-related pattern are *Amazon\_employee\_access* and *KDDCup09\_appetency*, whose poor performance cannot be explained solely by dataset size.

#### D.4 ADDITIONAL EXPERIMENT RESULTS: BAYESIAN REGRET

In this section, we present the complete Bayesian regret results. Figures 22 to 24 show the 1D experiments, and Figures 25 to 27 show the 8D experiments. Each figure corresponds to one cost setting (uniform, linear or periodic) and three values of the cost-scaling factor,  $\lambda = 10^{-1}, 10^{-2}, 10^{-3}$ . In all of the experimental results, we observe that PBGI/LogEIPC acquisition function + PBGI/LogEIPC stopping achieves cost-adjusted regret that is not only competitive with the baselines, but is also competitive regarding the *best in hindsight* fixed iteration stopping and often competitive even comparing to *hindsight optimal* stopping. These results indicate that our automatic stopping rule can replace manual selection of stopping times without loss in performance. Figures 22 to 27 also show that our PBGI/LogEIPC stopping rule outperforms other baselines when the cost-scaling factor  $\lambda$  is large, indicating that it's an especially suitable stopping criteria when evaluation is expensive.

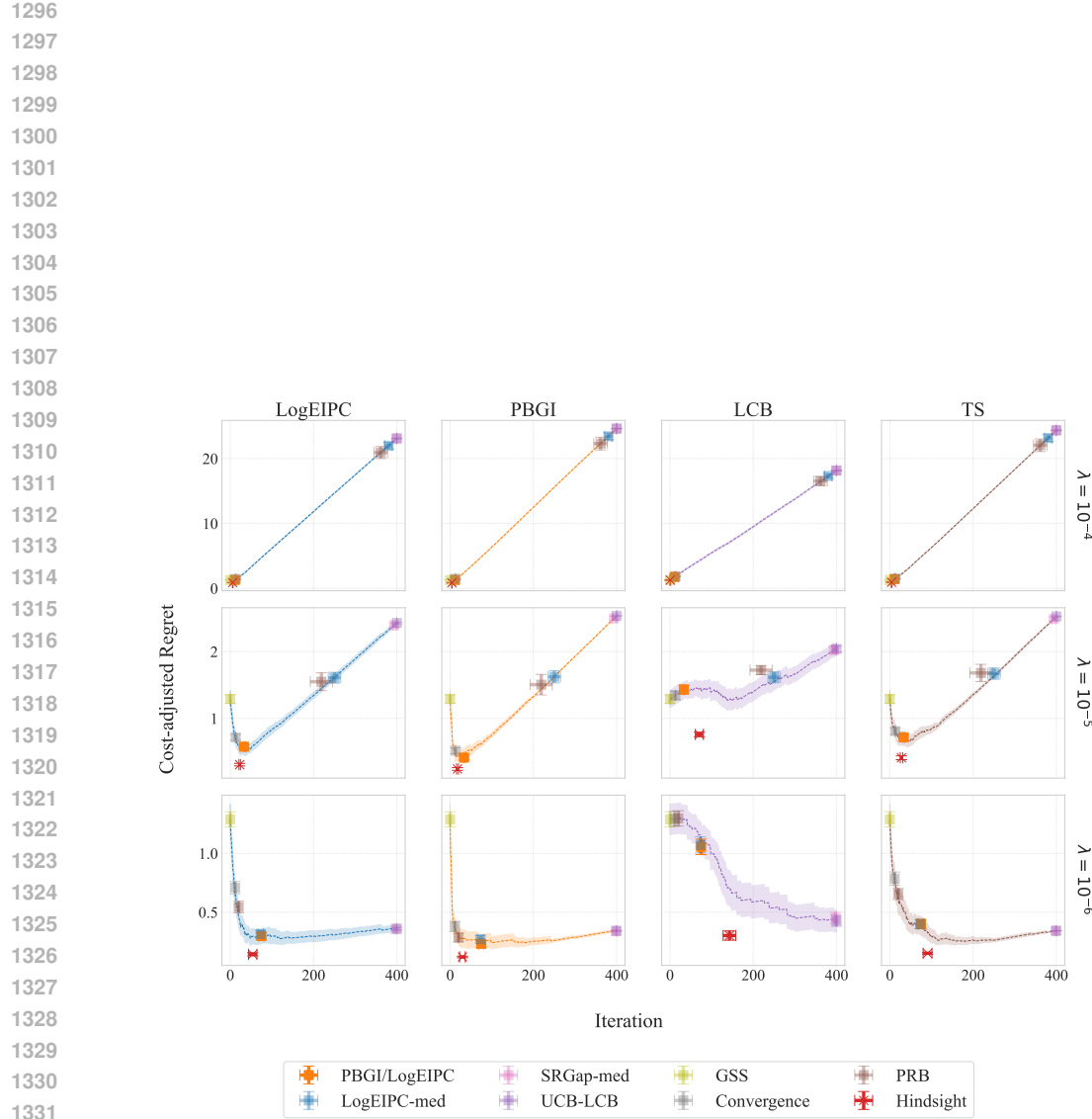


Figure 14: Comparison of cost-adjusted simple regret across acquisition function and stopping rule pairs on the *cifar10-valid* dataset. The objective function is the validation error, and the evaluation cost is the proxy runtime, scaled by three different cost-scaling factors  $\lambda = 10^{-4}, 10^{-5}, 10^{-6}$ . We can see that the PBGI/LogEIPC stopping rule consistently achieves the best cost-adjusted regret when paired with the LogEIPC, PBGI, or TS acquisition function, particularly with PBGI. These pairs not only approach the hindsight optimal adaptive stopping but also perform comparably to the hindsight optimal fixed-iteration stopping.

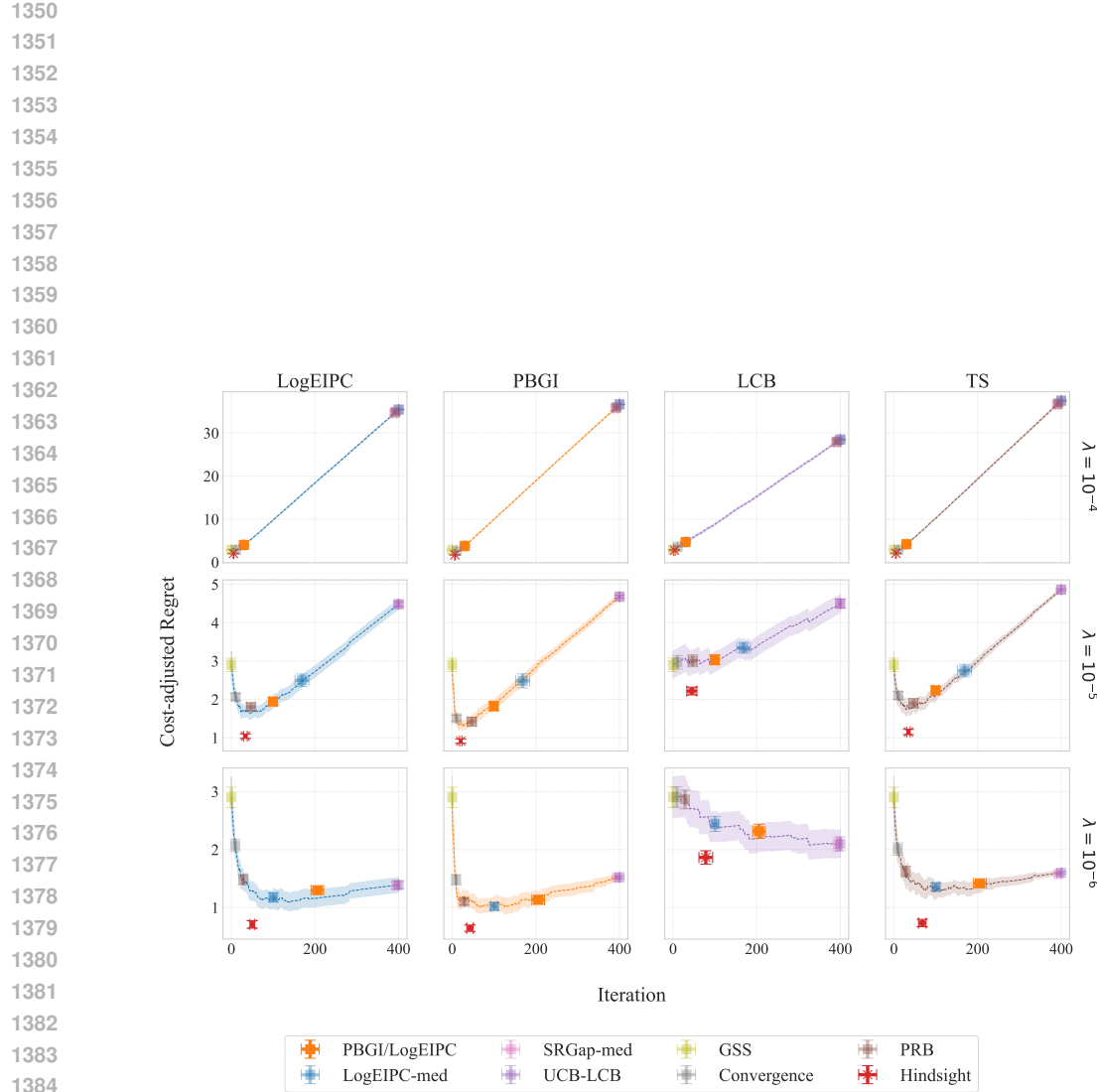


Figure 15: Comparison of cost-adjusted simple regret across acquisition function and stopping rule pairs on the *cifar100* dataset. The objective function is the validation error, and the evaluation cost is the proxy runtime, scaled by three different cost-scaling factors  $\lambda = 10^{-4}, 10^{-5}, 10^{-6}$ . The PBGI/LogEIPC stopping rule remains competitive at  $\lambda = 10^{-4}$  and  $10^{-6}$ , though not always the best. At  $\lambda = 10^{-5}$ , unlike in most experiments, it stops noticeably late (though still outperforming several other rules), even when paired with its matching acquisition function. By Lemma 1, under model match, the PBGI/LogEIPC rule with the corresponding acquisition function should never incur negative expected cost-adjusted regret before stopping. The suboptimal behavior observed here points to significant model mismatch on the *cifar100* dataset.

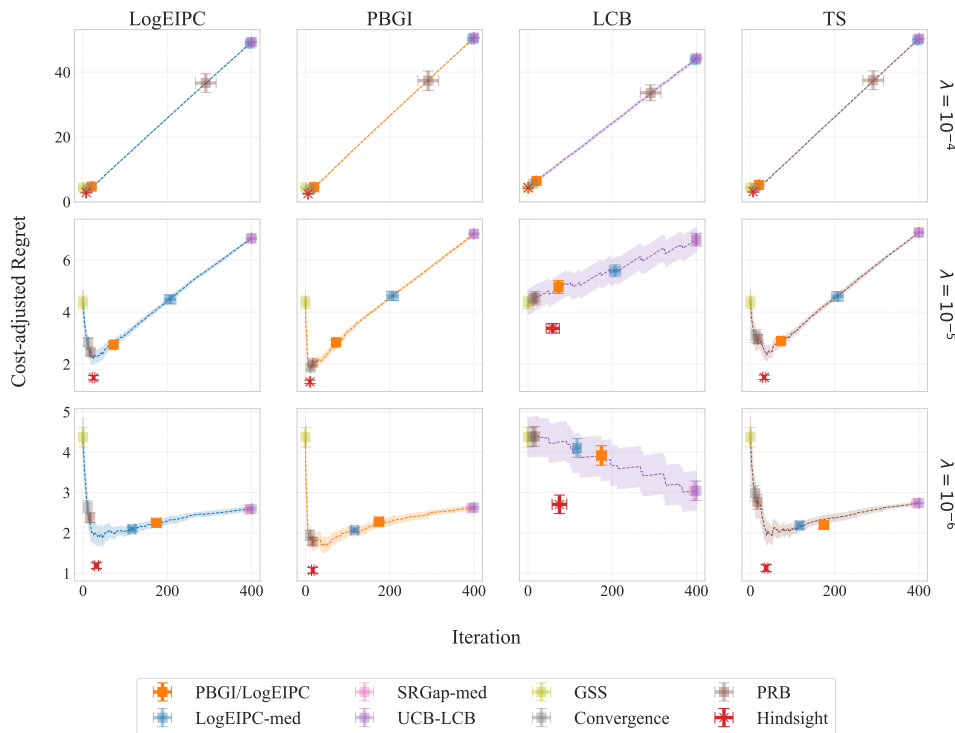
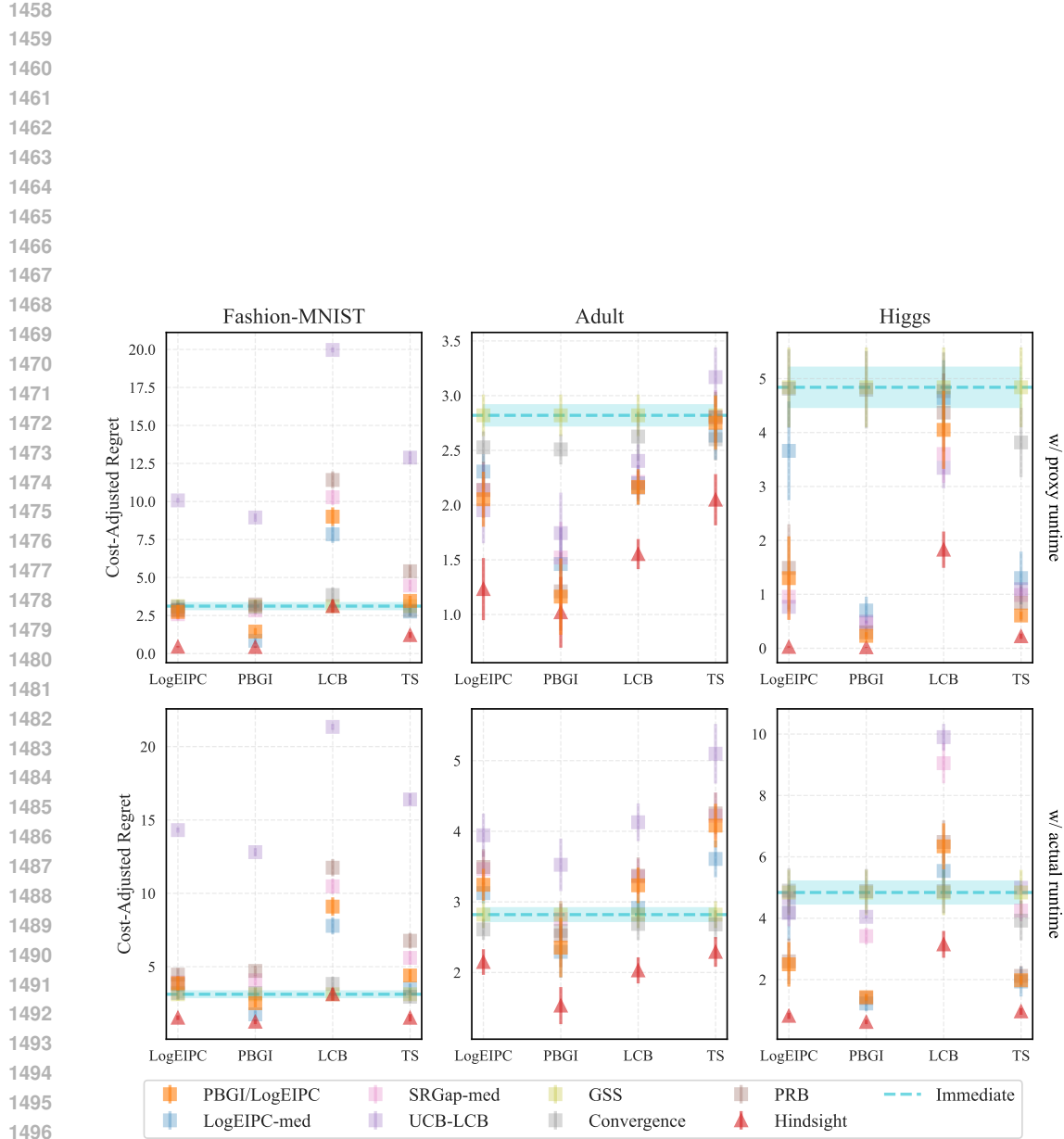


Figure 16: Comparison of cost-adjusted simple regret across acquisition function and stopping rule pairs on the *ImageNet16-120* dataset. The objective function is the validation error, and the evaluation cost is the proxy runtime, scaled by three different cost-scaling factors  $\lambda = 10^{-4}, 10^{-5}, 10^{-6}$ . The PBGI/LogEIPC stopping rule remains competitive at  $\lambda = 10^{-4}$  and  $10^{-6}$ , though not always the best. At  $\lambda = 10^{-5}$ , unlike in most experiments, it stops noticeably late (though still outperforming several other rules), even when paired with its matching acquisition function. By Lemma 1, under model match, the PBGI/LogEIPC rule with the corresponding acquisition function should never incur negative expected cost-adjusted regret before stopping. The suboptimal behavior observed here points to significant model mismatch on the *ImageNet16-120* dataset.



1498      Figure 17: Comparison of cost-adjusted simple regret on three LCBench datasets with  $\lambda = 10^{-4}$ ,  
1499      using scaled proxy runtime vs. scaled actual runtime as evaluation cost. While our PBGI/LogEIPC  
1500      stopping rule performs slightly worse under actual runtime (e.g., dropping from best to second-best  
1501      on the *higgs* dataset), likely due to cost model mismatch, it remains close to the hindsight optimal in  
1502      all cases.

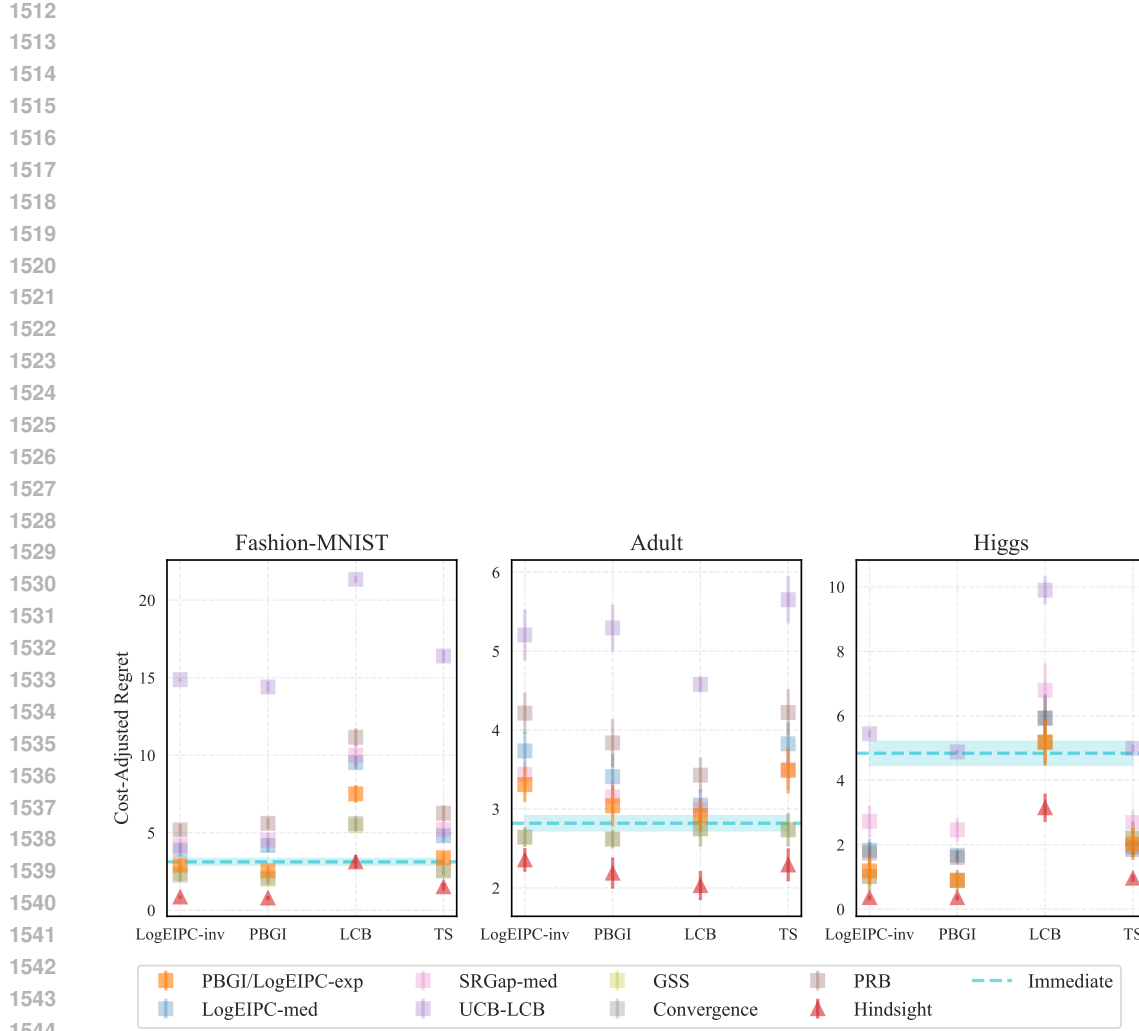


Figure 18: Cost-adjusted simple regret across acquisition function and stopping rule pairs under the unknown-cost setting on LC Bench with  $\lambda = 10^{-4}$ . Our PBGI/LogEIPC stopping rule remains close to the hindsight optimal when paired with the LogEIPC-exp or PBGI acquisition function, sometimes slightly worse than heuristics such as GSS and Convergence. It is also slightly worse than Immediate on *Adult*, likely due to a cost-model mismatch in the unknown-cost setting.

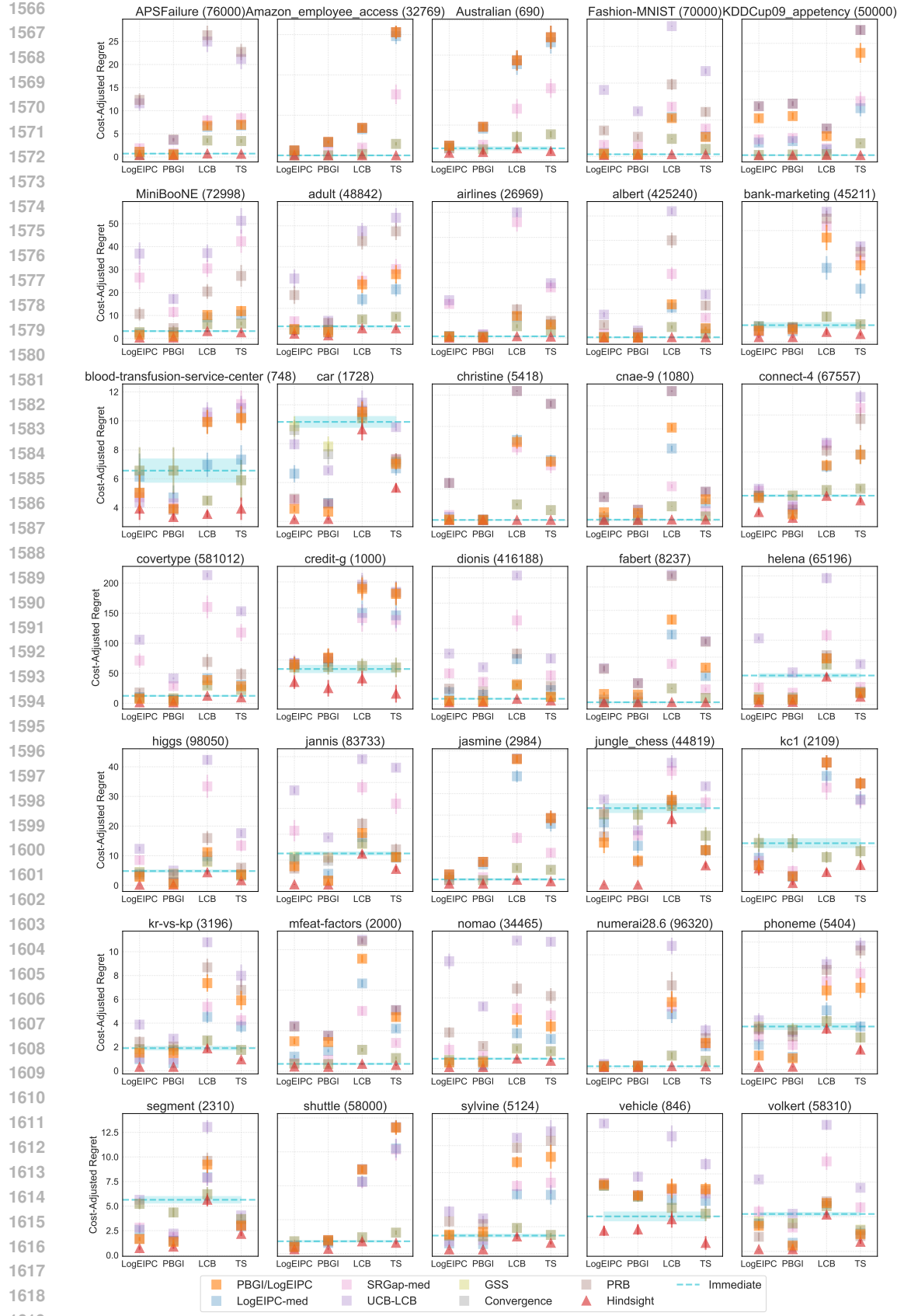


Figure 19: Cost-adjusted simple regret of all 35 LCBench datasets when  $\lambda = 10^{-3}$ .

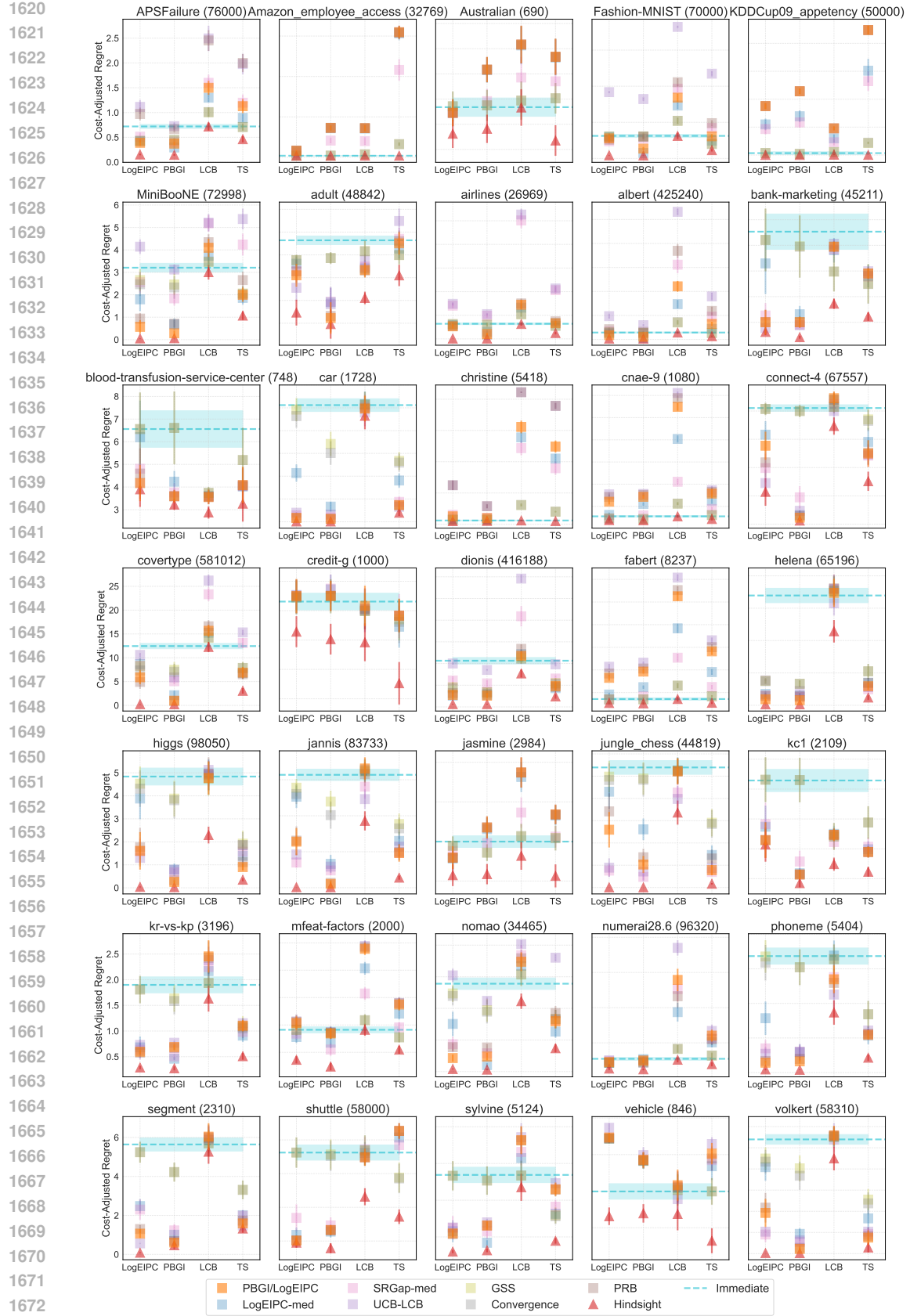
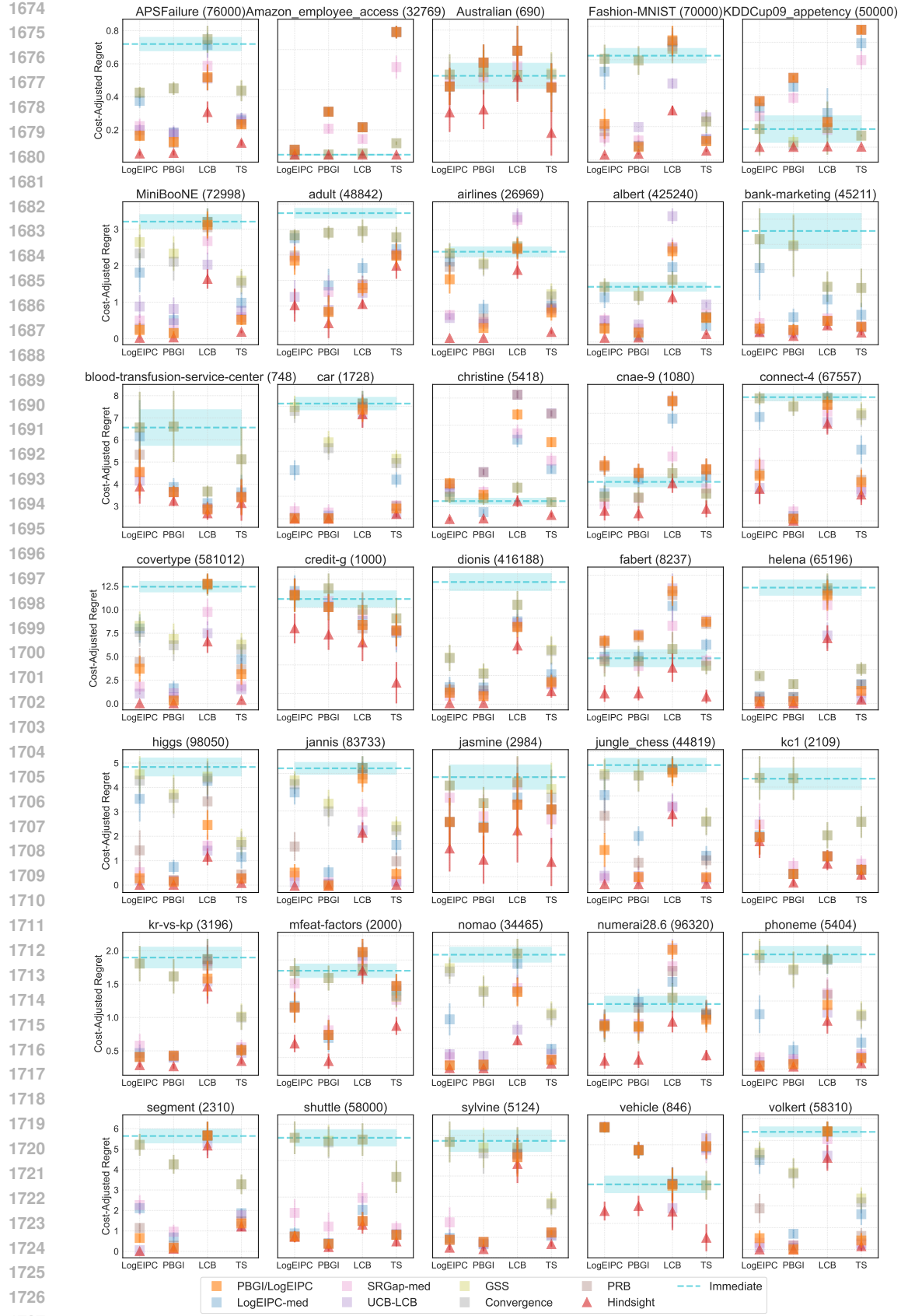


Figure 20: Cost-adjusted simple regret of all 35 LCBench datasets when  $\lambda = 10^{-4}$ .

Figure 21: Cost-adjusted simple regret of all 35 LCBench datasets when  $\lambda = 10^{-5}$ .

1728

1729

1730

1731

1732

1733

1734

1735

1736

1737

1738

1739

1740

1741

1742

1743

1744

1745

1746

1747

1748

1749

1750

1751

1752

1753

1754

1755

1756

1757

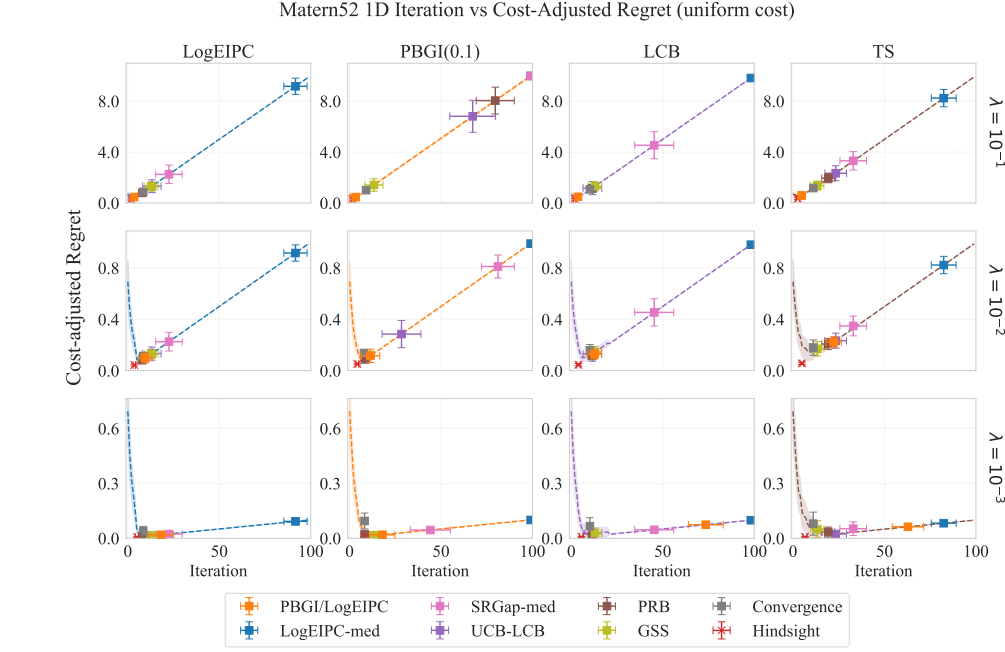


Figure 22: Comparison of cost-adjusted simple regret across acquisition function and stopping rule pairs in the 1D Bayesian regret experiments, with cost-scaling factor  $\lambda = 10^{-1}, 10^{-2}, 10^{-3}$  and under uniform cost. The dashed line in each subplot represent fixed iteration stopping (e.g., the y-axis value of the line at iteration 50 represent the cost-adjusted regret when always stop at iteration 50).

1758

1759

1760

1761

1762

1763

1764

1765

1766

1767

1768

1769

1770

1771

1772

1773

1774

1775

1776

1777

1778

1779

1780

1781

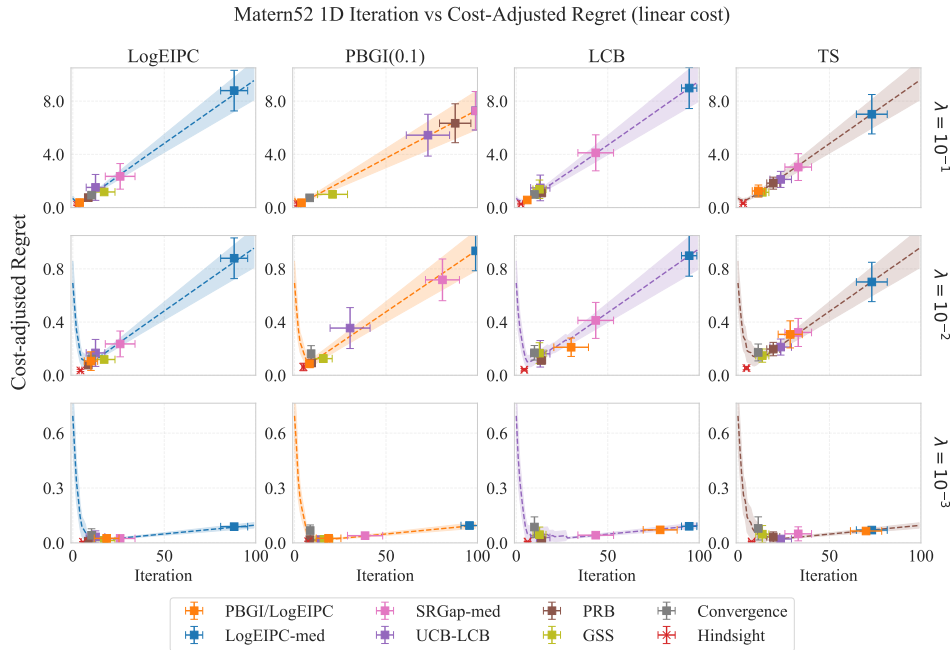
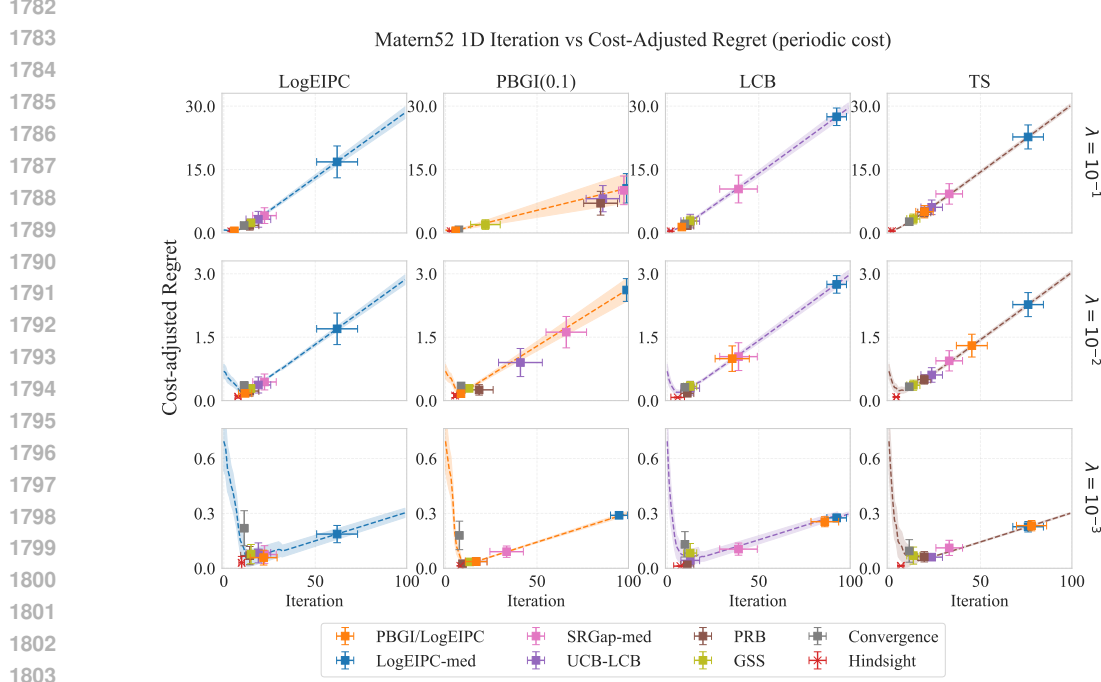
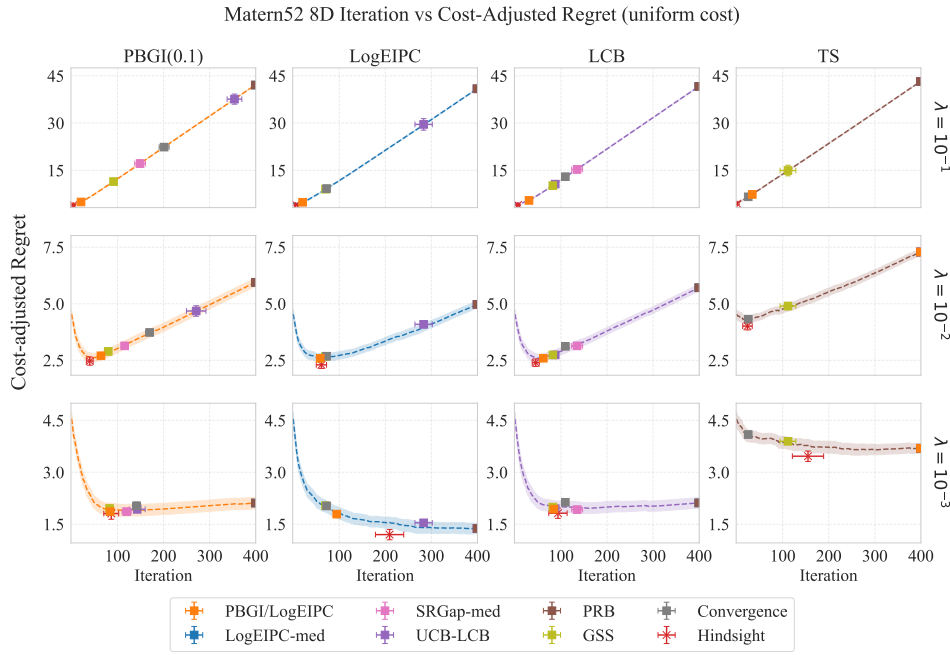


Figure 23: Comparison of cost-adjusted simple regret across acquisition function and stopping rule pairs in the 1D Bayesian regret experiments, with cost-scaling factor  $\lambda = 10^{-1}, 10^{-2}, 10^{-3}$  and under linear cost. The dashed line in each subplot represent fixed iteration stopping (e.g., the y-axis value of the line at iteration 50 represent the cost-adjusted regret when always stop at iteration 50).



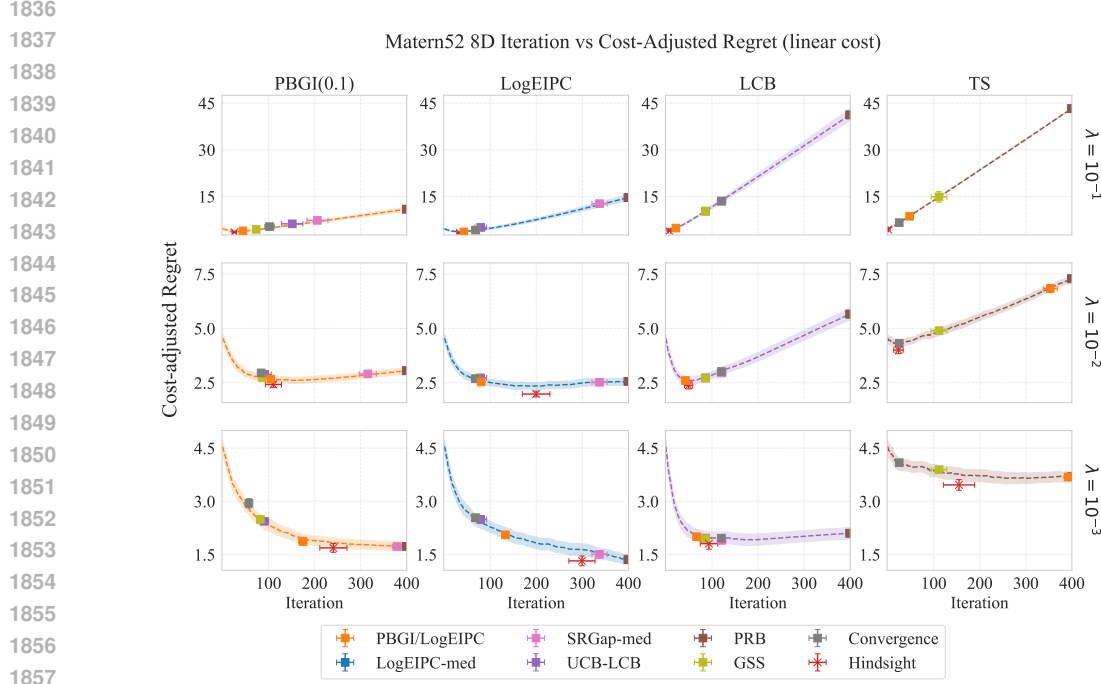
1804  
1805  
1806  
1807  
1808  
1809  
1810  
1811  
1812  
1813  
1814  
1815  
1816  
1817  
1818  
1819  
1820  
1821  
1822  
1823  
1824  
1825  
1826  
1827  
1828  
1829  
1830  
1831

Figure 24: Comparison of cost-adjusted simple regret across acquisition function and stopping rule pairs in the 1D Bayesian regret experiments, with cost-scaling factor  $\lambda = 10^{-1}, 10^{-2}, 10^{-3}$  and under periodic cost. The dashed line in each subplot represent fixed iteration stopping (e.g., the y-axis value of the line at iteration 50 represent the cost-adjusted regret when always stop at iteration 50).

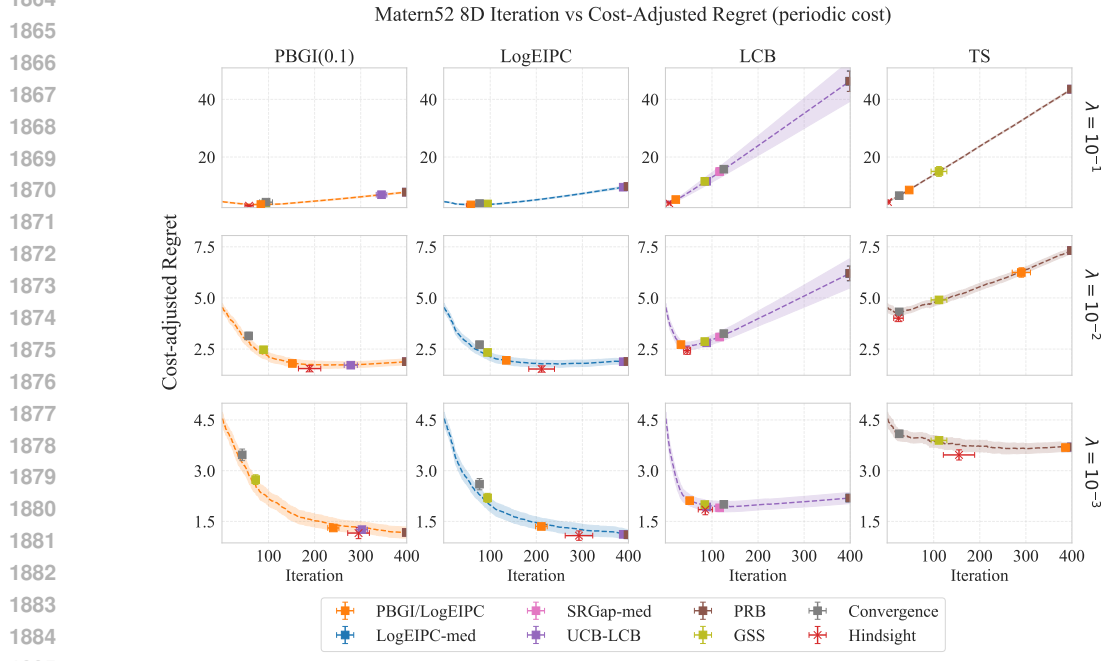


1832  
1833  
1834  
1835

Figure 25: Comparison of cost-adjusted simple regret across acquisition function and stopping rule pairs in the 8D Bayesian regret experiments, with cost-scaling factor  $\lambda = 10^{-1}, 10^{-2}, 10^{-3}$  and under uniform cost. The dashed line in each subplot represent fixed iteration stopping (e.g., the y-axis value of the line at iteration 50 represent the cost-adjusted regret when always stop at iteration 50).



1858 Figure 26: Comparison of cost-adjusted simple regret across acquisition function and stopping rule  
1859 pairs in the 8D Bayesian regret experiments, with cost-scaling factor  $\lambda = 10^{-1}, 10^{-2}, 10^{-3}$  and  
1860 under linear cost. The dashed line in each subplot represent fixed iteration stopping (e.g., the y-axis  
1861 value of the line at iteration 50 represent the cost-adjusted regret when always stop at iteration 50).  
1862  
1863  
1864



1885 Figure 27: Comparison of cost-adjusted simple regret across acquisition function and stopping rule  
1886 pairs in the 8D Bayesian regret experiments, with cost-scaling factor  $\lambda = 10^{-1}, 10^{-2}, 10^{-3}$  and  
1887 under periodic cost. The dashed line in each subplot represent fixed iteration stopping (e.g., the y-axis  
1888 value of the line at iteration 50 represent the cost-adjusted regret when always stop at iteration 50).  
1889